ELSEVIER

Coordination Chemistry Reviews
168 (1998) 233–271

COORDINATION CHEMISTRY REVIEWS

Ru(II) polypyridine complexes with a high oxidation power. Comparison between their photoelectrochemistry with transparent SnO_2 and their photochemistry with desoxyribonucleic acids

Isabelle Ortmans [1], Cécile Moucheron, Andrée Kirsch-De Mesmaeker [2] *

Chimie Organique Physique, Université Libre de Bruxelles, CP 160/08, 50 avenue F.D. Roosevelt, 1050 Brussels, Belgium

Received 2 July 1997; accepted 15 September 1997

Contents

* *Corresponding author. Tel.: +32 650 3017 2048; Fax: +32 650 3606; e-mail: akirsch@ulb.ac.be*

[1] Aspirant at the FNRS (Belgium).

[2] Director of Research at the FNRS (Belgium).

PII S0010-8545(97)00070-2

Abstract

The compounds which are discussed in the present review are highly oxidizing Ru(II) complexes, based on various polyazaaromatic ligands, and acting as efficient electron *acceptors* in the excited state. The photoinduced charge transfer process and the following associated kinetic steps are characterized for the whole series of complexes by quite different techniques and methods. Thus their behaviour in the presence of reductants such as hydroquinone and mononucleotides (guanosine-5′-monophosphate and adenosine-5′-monophosphate) are examined by flash photolysis, spectroelectrochemistry and photoelectrochemistry. It is explained how the light-initiated electron transfer process can be applied for spectral supersensitization of wide band gap SnO_2 semiconductor electrodes. Moreover, it is shown that such a knowledge of the behaviour of these photoredox reactions leads to interesting applications of these oxidizing complexes in a biological area, i.e. for the study of nucleic acids. Thus it is illustrated how these compounds can be used as promising photoreagents of DNA. The easy modulation of their size and shape, and their irreversible anchoring on the DNA bases, triggered by the reductive photoelectron transfer process from the guanine bases to the excited complex, allow one to regard these complexes as attractive molecular tools for DNA study and maybe as future possible drugs activatable under visible light. © 1998 Elsevier Science S.A.

Keywords: Polypyridine Ru(II) complexes; Photoelectrochemistry; Spectroelectrochemistry; DNA interaction; DNA photocleavages; DNA photoadducts

1. Introduction

Many reviews have been devoted to Ru(II) complexes where the interesting properties of their MLCT (metal to ligand charge transfer) excited states have been highlighted. This field of extensive research has induced the development of several applications based on these compounds in quite different areas. For example Ru(II) polypyridine complexes have been used as photosensitizers for the splitting of water into elemental hydrogen and oxygen [1–9] and for the spectral sensitization of wide band gap semiconductor electrodes in photoelectrochemical cells [10–23]. These important developments in solar energy conversion and storage include also the design of molecular devices mimicking antenna systems [24,25]. More recently Ru(II) complexes have been studied as sensors in optrodes probing different kinds of analytes [26] and as photoprobes and photoreagents of biological molecules such as DNA [27–29]. They have also been chemically attached to synthetic oligodeoxynucleotides as specific luminescent probes [30–32] or photoreagents [33] of particular DNA sequences in order to inhibit specific gene functions. The complexes which have been tested in these various applications are of different types, they extend from monometallic to polymetallic species or from monofunctional to polyfunctional compounds. Examples of such complexes will be discussed later.

The most exploited properties of these Ru(II) compounds are their photoredox behaviour responsible for photoinduced electron transfer reactions. It is striking to observe that, in most systems where the elementary photoelectron transfer process has been studied, the Ru(II) complex acts as an efficient electron donor. The well-

known $Ru(bpy)_3^{2+}$ (bpy = 2,2′-bipyridine) behaves indeed as a powerful reducing agent in the excited state. Therefore, in photoelectrochemistry as explained later, the excited state of $Ru(bpy)_3^{2+}$ and its derivatives is able to inject an electron into the conduction band of high band gap n-type semiconductor oxides.

In this article in contrast, the discussion will focus on Ru(II) complexes which behave as electron acceptors, i.e. as powerful oxidants, in the excited ^{3}MLCT state. These complexes are formed with polyazaaromatic ligands (Fig. 1) containing additional unchelated nitrogen atoms in the aromatic rings: these supplementary nitrogen atoms induce significant changes in the photophysics and redox properties of the metal compounds, as reported previously for Ru(II) complexes based on bpz (bpz = 2,2′-bipyrazine), bpm (bpm = 2,2′-bipyrimidine) [34–36] and TAP (TAP = 1,4,5,8-tetraazaphenanthrene) ligands [37].

Two applications of these highly photo-oxidizing complexes will be reviewed: the first one corresponds to their use in photoelectrochemistry with transparent SnO_2, while the second application, of biological interest, involves DNA studies. In both cases, we will discuss on the one hand, the striking similarities in the behaviour characterizing the photo-oxidizing Ru(II) compounds and, on the other hand, the differences as compared to all the other complexes studied in the literature. These usually behave as reducing agents in the excited state. In other words, the goal of this work is to show for this series of complexes, the similarity in the different elemental processes taking place at a semiconductor | solution interface in photoelectrochemistry (PEC) and in the microenvironment of a DNA double helix. Once these elemental processes have been characterized, it is easy to extrapolate the behaviour from one complex to the other in the same application, or from PEC to DNA studies for the same complex. While reviewing these two applications, we will stress the influence of a supplementary important parameter for the DNA studies, i.e. the shape and morphology of the metal compounds. Indeed this factor plays an essential role in the interaction of the rigid octahedral Ru(II) complexes with DNA. As the shapes and the photoredox properties can easily be modulated, this represents a major advantage of the Ru(II) compounds as photoprobes and photoreagents of DNA.

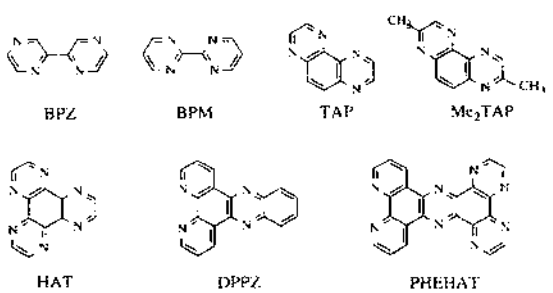

Fig. 1. Structure of different polyazaaromatic ligands. BPZ = 2,2′-bipyrazine; BPM = 2,2′-bipyrimidine; TAP = 1,4,5,8-tetraazaphenanthrene; $TAPMe_2$ = 2,7-dimethyl-1,4,5,8-tetraazaphenanthrene; HAT = 1,4,5,8,9,12-hexaazatriphenylene; DPPZ = dipyrido[3,2-*a*:2′,3′-*c*]phenazine; PHEHAT = 1,10-phenanthrolino-[5,6-*b*]1,4,5,8,9,12-hexaazatriphenylene.

Having defined the focus of this work, the series of complexes which will be reviewed is rather restrictive. The list is given in Table 1 where the redox properties of the complexes in the ground and excited states are compared to the electrochemical properties of the well-known $Ru(bpy)_3^{2+}$.

From inspection of Table 1, we can conclude that all the polyazaaromatic complexes are more oxidant in their ground and excited states than $Ru(bpy)_3^{2+}$. The monometallic TAP compounds $Ru(bpy)_i(phen)_iTAP_3^{2+}$; (phen = 1,10-phenanthroline; $i = 0,1,2$) have their first ground state reduction wave shifted positively by about 0.5–0.6 V compared to $Ru(bpy)_3^{2+}$ and the oxidation power increases with the

Table 1
Oxidation (E_{ox}) and reduction potentials (E_{red}) of a series of Ru(II) complexes, together with the corresponding oxidation (E^*_{ox}) and reduction potentials (E^*_{red}) in the excited ^{3}MLCT state [data vs SCE]

Complex	E_{ox}	E_{red}	E^*_{ox} [a]	E^*_{red} [a]	Reference
$Ru(HAT)_3^{2+}$	+2.07	−0.62	−0.01	+1.46	[39]
$Ru(HAT)_2(TAP)^{2+}$	+2.03	−0.64	−0.04	+1.43	[39]
$Ru(TAP)_2(HAT)^{2+}$	+2.02	−0.68	−0.02	+1.36	[39]
$Ru(TAP)_3^{2+}$	+1.94	−0.75	−0.12	+1.32	[37]
$Ru(BPZ)_3^{2+}$	+1.86	−0.86	−0.20	+1.27	[3]
$Ru(Me_2TAP)_3^{2+}$	+1.80	−0.84	−0.28	+1.24	[42]
$Ru(HAT)_2(phen)^{2+}$	+1.86	−0.66	−0.03	+1.23	[46]
$Ru(TAP)_2(DPPZ)^{2+}$	+1.77	−0.80	−0.18	+1.15	[126]
$Ru(BPZ)_2(DPPZ)^{2+}$ [b]	+1.77	−0.78	−0.15	+1.14	[125]
$Ru(HAT)_2(bpy)^{2+}$	+1.79	−0.76	−0.08	+1.12	[39]
$Ru(bpy)(TAP)(HAT)^{2+}$	+1.78	−0.75	−0.08	+1.11	[39]
$Ru(TAP)_2(bpy)^{2+}$	+1.70	−0.83	−0.19	+1.06	[46]
$Ru(TAP)_2(phen)^{2+}$	+1.73	−0.83	−0.16	+1.06	[46]
$Ru(phen)_2(PHEHAT)^{2+}$ [c,d]	+1.35	−0.84	−0.52	+1.03	[38]
$Ru(bpy)_2(DPPZ)^{2+}$ [c,d]	+1.24	−1.02	−0.75	+0.97	[41,125]
$Ru(phen)_2(DPPZ)^{2+}$ [c,d]	+1.30	−1.00	−0.67	+0.97	[38]
$Ru(bpy)_2(TAP)^{2+}$	+1.51	−0.88	−0.23	+0.86	[37]
$Ru(phen)_2(HAT)^{2+}$	+1.53	−0.86	−0.16	+0.83	[38]
$Ru(bpy)_2(HAT)^{2+}$	+1.56	−0.84	−0.11	+0.83	[39]
$Ru(bpy)_3^{2+}$	+1.28	−1.35	−0.73	+0.66	[37]
$[Ru(bpy)_2]_2HAT^{4+}$ [c]	+1.53	−0.49			[39]
$[Ru(phen)_2]_2HAT^{4+}$ [e]	+1.52	−0.49	+0.01	+1.02	[39,40]

[a] Values for the oxidation (E^*_{ox}) and reduction (E^*_{red}) potentials of the excited complexes estimated from the oxidation (E_{ox}) and reduction (E_{red}) potentials in the ground state (measured by cyclic voltammetry in acetonitrile) and from the energy of the emission maximum (ΔE_{max}) in water.

[b] The redox potentials in the excited state have been estimated with a ΔE_{max} value corresponding to the uncorrected emission maximum in water.

[c] As the complex does not luminesce in water, the redox potentials in the excited state have been estimated with the energy of the emission maximum in acetonitrile.

[d] The orbitals involved in the spectroscopic and redox processes are not the same and formally, the redox potentials in the excited state are not correct (see comments in the text).

[e] As the emission maximum cannot be determined because it is too bathochromic ($\lambda_{max} > 800$ nm), the redox potentials in the excited state have not been estimated.

[f] The redox potential values have been measured for each stereoisomer and do not change from one isomer to the other [40].

number of π-deficient TAP ligands in this series. The HAT ligand (HAT = 1,4,5,8,9,12-hexaazatriphenylene) induces the same behaviour on the corresponding complexes $Ru(bpy\ phen)_i HAT^{2+}_3$ ($i = 0,1,2$). The anodic shift of the first reduction wave as compared to $Ru(bpy)^{2+}_3$ is however smaller for the $Ru(bpy\ phen)_2DPPZ^{2+}$ compounds (DPPZ = dipyrido[3,2-*a*:2′,3′-*c*]phenazine). Interestingly the first reduction wave for the PHEHAT complex (PHEHAT = 1,10-phenanthrolino[5,6-*b*]1,4,5,8,9,12-hexaazatriphenylene) appears at the same potential as for $Ru(phen)_2HAT^{2+}$, indicating that on reduction, the process is controlled by the HAT fragment of the PHEHAT ligand [38]. The first reduction wave of the bimetallic HAT complexes is positively shifted with respect to the corresponding wave of the related monometallic compounds. This effect may be attributed to the stabilization of low-lying π* orbitals upon multicomplexation of the bridging HAT ligand [39]. Recently it has been shown [40] that the redox potential values of these dinuclear complexes, containing ancillary bpy or phen ligands, do not change from one stereoisomer to the other (i.e. from the *racemic* Δ Δ, λ λ, to the *meso* Δ λ).

The ground state oxidation potentials characterizing the monometallic TAP and HAT complexes and the bimetallic HAT compounds are also positively shifted in comparison with the value obtained for $Ru(bpy)^{2+}_3$. The positive shift is however significantly smaller for the monometallic PHEHAT complex, indicating that the PHEHAT ligand exhibits, in contrast to the reduction process, the same properties as the phen ligand as far as the oxidation of the metal centre is concerned [38]. The same conclusion may be reached for the DPPZ ligand in the monometallic $Ru(bpy\ phen)_2DPPZ^{2+}$ compounds [41].

The redox potentials for the excited state have been estimated on the basis of the energy of the emission maximum ($E^*_{red} = E_{red} + \Delta E_{zmax}$; $E^*_{ox} = E_{ox} - \Delta E_{zmax}$). It is obvious from Table 1 that the monometallic TAP and HAT complexes and the bimetallic $[Ru(phen)_2]_2HAT^{4+}$ behave as poor excited state reductants. The excited state reduction potentials confirm on the other hand the high oxidation power of all the polyazaaromatic complexes in their ^{3}MLCT excited state. The complexes based on three TAP HAT π-acceptor ligands show the strongest oxidation powers. For the $Ru(phen)_2PHEHAT^{2+}$ and $Ru(bpy\ phen)_2DPPZ^{2+}$ compounds, the estimation of the redox potentials in the excited state is not formally correct as, for those particular complexes, the PHEHAT or DPPZ orbitals involved in the spectroscopic and redox processes are not the same [38,41]. The values mentioned in Table 1 correspond therefore to an approximation which will be useful for the study of these compounds in the presence of nucleic acids (see below).

In summary, throughout this review, the primary photoinduced process responsible for semiconductor oxide supersensitization and irreversible damage caused to DNA is examined. This elementary photoelectron transfer corresponds to the reaction (Eq. (1))

$$C^* + D \xrightarrow{k_{et}} C^- + D^+ \qquad (1)$$

where C represents one of the Ru(II) compounds listed in Table 1, while the

reductive quencher D corresponds to hydroquinone, to mononucleotides, or even to synthetic polynucleotides or natural DNA.

The photo-oxidative behaviour of the complexes is first examined in the presence of hydroquinone and mononucleotides, using $Ru(TAP)_3^{2+}$ as a model compound. The detection and mechanistic study of the monoreduced complex C^+ generated by the elementary photoinduced process (Eq. (1)) are surveyed on the basis of various experimental approaches including flash photolysis and spectroelectrochemical techniques. The results obtained for the $Ru(TAP)_3^{2+}$–hydroquinone system are then used as a basis to elucidate the behaviour at an SnO_2 semiconductor electrode and to correlate the corresponding photoelectrochemical data with the flash photolysis results obtained in solution studies. The final part of the review is dedicated to the study of the photoelectron transfer in the presence of DNA and to the description of DNA reactions induced by this process.

2. Spectroscopic and kinetic evidence for the elementary photoinduced electron transfer process

The photoredox behaviour of the highly oxidizing Ru(II) complexes listed in Table 1 has been examined in the presence of several reductants corresponding to hydroquinone (H_2Q) [42–44] and various mononucleotides including GMP and AMP (GMP = guanosine-5′-monophosphate, AMP = adenosine-5′-monophosphate) [45,46]. Considering the reducing power of these reductants ($E_{ox}H_2Q = +0.53$ V vs SCE in a neutral medium [47]; $E_{ox}GMP = +0.82$ V vs SCE at pH 7 [48]) and the oxidizing power of the excited Ru(II) complexes (Table 1, E^*_{red}), a photoelectron transfer process is expected to occur from H_2Q and GMP to most excited Ru(II) compounds of Table 1. The formation of a monoreduced complex according to reaction (Eq. (1)) has indeed been observed for this series of compounds illuminated in the presence of H_2Q and/or GMP. When the reductive quencher corresponds to AMP, only the most oxidizing excited complexes ($E^*_{red} \geq 1.32$ V vs SCE [46]) are photoreduced, in agreement with the higher oxidation potential of this mononucleotide.

The results from the various experimental techniques which allow the detection and characterization of the monoreduced complex resulting from reaction (Eq. (1)) are described for the $Ru(TAP)_3^{2+}$ model compound and they are more briefly overviewed for the other complexes. In order to highlight the photoelectrochemical behaviour of the C*+D system at a semiconductor electrode and correlate the corresponding PEC results with the data obtained from spectroscopic and other kinetic methods, we will first survey the results obtained with the non-photoelectrochemical techniques. These data will also be used as a basis to elucidate the photoreactivity of the Ru(II) complexes versus DNA.

2.1. Luminescence quenching experiments

The first experimental evidence for the occurrence of process (Eq. (1)) has been found in the luminescence quenching of the Ru(II) complexes upon addition of the

reducing agent. The $Ru(TAP)_3^{2+}$ model compound has been studied in the presence of hydroquinone and mononucleotides (Table 2). For the latter, the highest quenching rate constant value is obtained with GMP, that is when the exergonicity of the photoinduced electron transfer process is the largest considering the various $Ru(TAP)_3^{2+}$ mononucleotide systems. Whereas quenching rate constants can be obtained with AMP, the luminescence quenching with TMP and CMP (TMP= thymidine-5′-monophosphate, CMP=cytosine-5′-monophosphate) is negligible, indicating that those two bases are not oxidized by the excited $Ru(TAP)_3^{2+*}$. For the other complexes discussed in this review, it has been shown that the emission of many of them is quenched by GMP (Table 2).

The plot of the logarithms of the corresponding quenching rate constants as a function of the reduction potential of the excited complexes (Fig. 2) gives a curve typical for the quenching by an electron transfer process, where the plateau value corresponds to the most exergonic charge transfers which are diffusion controlled. These data, analyzed on the basis of the Marcus and Rehm-Weller equation, give a

Table 2
Luminescence quenching rate constants measured for a series of Ru(II) complexes in the presence of mononucleotides[a] and H_2Q

Complex	GMP		AMP[b]		H_2Q	
	k_q ($10^9 M^{-1} s^{-1}$)	Ref.	k_q ($10^9 M^{-1} s^{-1}$)	Ref.	k_q ($10^9 M^{-1} s^{-1}$)	Ref.
$Ru(HAT)_3^{2+}$	2.16	[46]	0.87	[46]		
$Ru(HAT)_2(TAP)^{2+}$	2.39	[46]	0.38	[46]		
$Ru(TAP)_2(HAT)^{2+}$	2.16	[46]	0.13	[46]		
$Ru(TAP)_3^{2+}$	2.20	[45,46]	0.12	[46]	4.9	[42]
$Ru(BPZ)_3^{2+}$	1.98	[46]	[c]			
$Ru(Me_2TAP)_3^{2+}$	1.74	[46]	[c]		5.2	[42]
$Ru(HAT)_2(phen)^{2+}$	1.85[e]	[46]	[c]			
$Ru(TAP)_2(DPPZ)^{2+}$	1.70	[126]	[c]			
$Ru(HAT)_2(bpy)^{2+}$	1.36	[46]	[c]			
$Ru(TAP)_2(bpy)^{2+}$	0.74	[46]	[c]			
$Ru(TAP)_2(phen)^{2+}$	0.98[e]	[46]	[c]			
$Ru(phen)_2(PHEHAT)^{2+}$	[d]		[d]			
$Ru(bpy)_2(TAP)^{2+}$	[c]	[46]	[c]		0.7	[44]
$Ru(phen)_2(HAT)^{2+}$	0.024	[46]	[c]			
$Ru(bpy)_2(HAT)^{2+}$	0.020	[46]	[c]			
$[Ru(phen)_2]_2HAT^{4+}$	0.3[f]	[59,130]	[c]		2.3	[44]

[a] The measurements in the presence of GMP and AMP were performed in buffered aqueous solution (0.1M phosphate buffer, pH 7).
[b] Only the most photo-oxidizing compounds ($E^*_{red} > 1.32$ V SCE, see Table 1) are photoreduced by AMP.
[c] The quenching rate constant was measured at pH 9 because of protonation of the excited state at lower pH.
[d] The complex does not emit in water.
[e] No luminescence quenching.
[f] Measurement at pH 9, no quenching at pH 7.

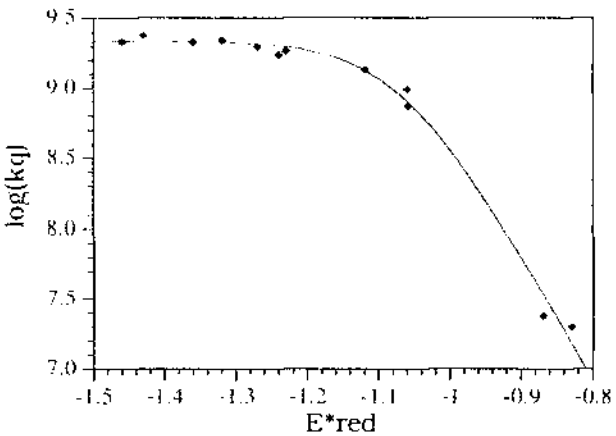

Fig. 2. Plot of the logarithm of the luminescence quenching rate constants k_q, measured in the presence of GMP, versus the excited state reduction potentials calculated for the complexes listed in Table 2 (adapted from Ref. [46]).

value for the oxidation potential of GMP which is in good agreement with the value obtained from pulse radiolysis experiments [46,49].

Further evidence for the photoinduced electron transfer process consists in detecting the production of the transient monoreduced complex C^{-}. This species thus needs to be clearly characterized, both spectroscopically and kinetically.

2.2. *Spectroscopic characterization*

The reductive quenching process (Eq. (1)) generates a one-electron-reduced species C^{-} which can be described as a ligand radical L$^{\bullet-}$ coordinated to a RuL_2 moiety ($[RuL_2L^{\bullet-}]^{+}$). The visible absorption spectrum of such a monoreduced complex is generally characterized by low energy bands resulting from ligand centred (LC) transitions localized on the reduced ligand. The ligand based reduction process is indeed known to induce a significant red shift of the corresponding ligand centred absorption bands [50–54]. This can easily be demonstrated by comparison of the C^{-} absorption spectrum with that of the free ligand reduced electrochemically. On the other hand MLCT transitions involving the reduced ligand are expected to shift to the blue as the π^* levels of these transitions increase in energy. In contrast, the MLCT bands towards the remaining intact ligands are much less affected as they are only slightly shifted to the red; these bands are therefore maintained in the visible region of the absorption spectrum of the monoreduced complex. These spectroscopic data have been obtained for several complexes of Table 1, from spectroelectrochemical measurements described below.

2.2.1. *Spectroelectrochemistry*

In a spectroelectrochemical experiment, the Ru(II) complex or the free ligand are electrochemically reduced at a potential corresponding to their first reduction wave

and visible absorption spectra of the electrolysis solution are recorded in the electrochemical cell as a function of reduction time. A typical spectroelectrochemical cell is made of an optically transparent gold minigrid working electrode, a platinum foil counter electrode and an AgCl reference electrode [55], maintained between two optical windows separated by a thin Teflon spacer. Reductive electrolysis is usually performed in acetonitrile in the presence of supporting electrolyte in deoxygenated solutions. The remaining traces of oxygen are generally reduced at the potentials applied to the working electrode (reduction of oxygen occurs at −0.78 V vs SCE in acetonitrile [56] and at −0.51 V vs SCE in water [57]). As the O_2 absorption appears below 340 nm [58], it does not disturb the detection of visible bands associated with the monoreduced complex or free ligand.

The evolution of the absorption spectrum of the free ligands TAP and HAT and of the absorption of $Ru(TAP)_3^{2+}$ and $[Ru(phen)_2]_2HAT^{4+}$ on electrochemical reduction is shown in Fig. 3 [44].

For the free reduced TAP, a new LC absorption band appears around 580 nm upon electrochemical reduction. In the case of the free HAT ligand, a band centred on 420 nm increases as a function of reduction time. There might be another absorption band characterizing the reduced HAT ligand in the 550–650 nm region, but the very low solubility of the HAT ligand in acetonitrile prevented the collection of clear data.

For the monometallic $Ru(TAP)_3^{2+}$ complex some decomposition is detected on electrochemical reduction. Complete recovery of the starting absorption upon application of a reverse bias (0 V vs SCE) to the working electrode is indeed observed only after short reduction times (≤2 min). The decomposition process corresponds probably to the loss of a ligand, as indicated by the occurrence of an absorption around 490–500 nm where complexes such as $Ru(TAP)_2X_2$ (X=Cl for example) absorb. Short electrolysis periods induce an absorption increase between 500 and 600 nm, in accord with the spectrum of the reduced TAP ligand. This absorption enhancement may consequently be attributed to the occurrence of LC transitions of the monoreduced TAP ligand in the corresponding reduced complex. There is on the other hand no complete disappearance of the MLCT Ru→TAP absorption bands in the 360–500 nm region, as the monoreduced complex still contains intact TAP ligands responsible for the remaining MLCT transitions. Upon reduction of $[Ru(phen)_2]_2HAT^{4+}$, the Ru-bridging HAT MLCT transitions decrease in the visible part of the spectrum and an absorption enhancement is observed between 400 and 500 nm, in agreement with the spectrum of HAT.

The absorption features of some monoreduced complexes of the TAP and HAT series have also been determined from pulsed radiolysis experiments. The corresponding results [45,46] are consistent with the spectroelectrochemical data.

2.2.2. *Laser flash photolysis*

Once the absorption features of the monoreduced complexes have been established on the basis of spectroelectrochemical and/or pulsed radiolysis data, the spectroscopic detection of transiently formed monoreduced complexes resulting from pro-

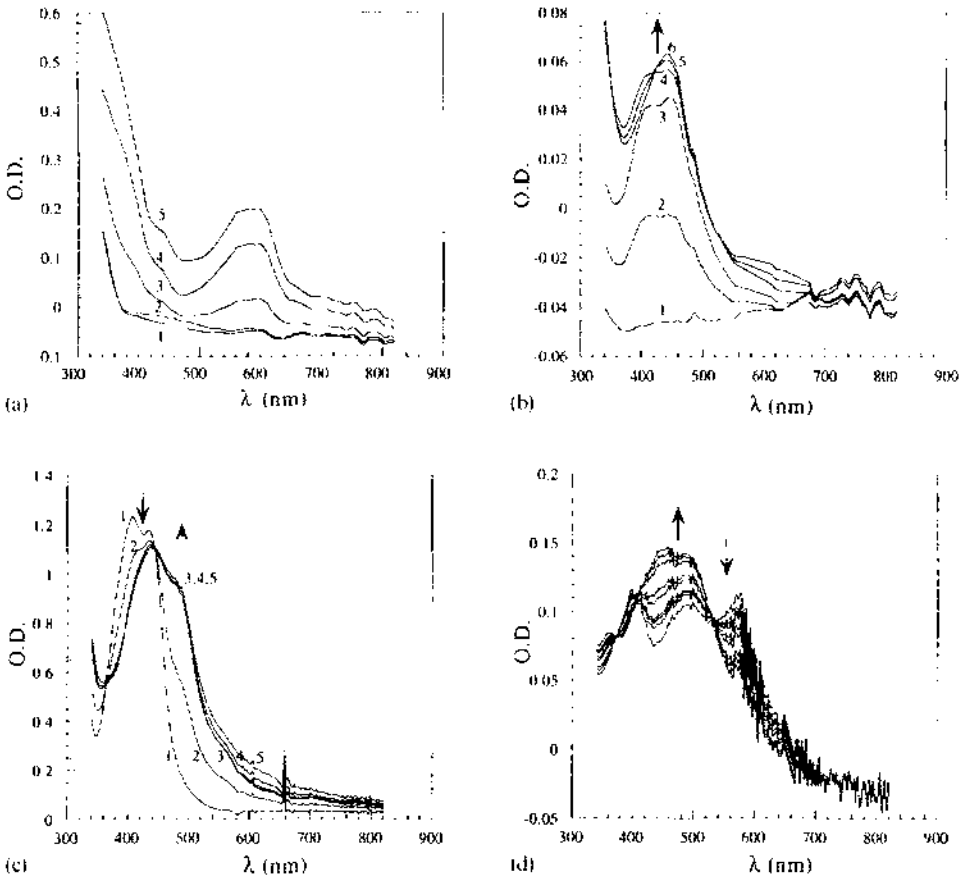

Fig. 3. Spectroelectrochemistry of free ligands and Ru(II) complexes at a gold minigrid electrode. The electrolysis was performed at a potential corresponding to the first reduction wave, in the presence of supporting electrolyte. (a) Free TAP ligand, 6 mM in acetonitrile, 0.1M NBu_4PF_6; spectra were recorded every 3 min. (b) Free HAT ligand, 0.1 mM in acetonitrile, 0.1M NBu_4PF_6; spectra were recorded at 2 min intervals. (c) $Ru(TAP)_3^{2+}$, 2.4 mM in acetonitrile, 0.1M NBu_4PF_6; spectra were recorded every 2 min. (d) $[Ru(phen)_2]_2HAT^{4+}$, 0.3 mM in water, pH 5.9, 0.1M $LiNO_3$; spectra were recorded at 2 min intervals [adapted from Ref. [46]].

cess (Eq. (1)) may be performed by flash photolysis experiments conducted in the presence of a reducing quencher.

In laser flash photolysis, the monoreduced complex is produced under pulsed irradiation in the presence of the reducing agent, and the absorbance change of the solution is monitored after the laser pulse, perpendicularly to the exciting beam. Just after the laser pulse, a differential transient absorption spectrum is obtained according to Eq. (1)

$$\Delta A(\lambda) = C_0 \cdot (\epsilon_{\text{C}} \quad -\epsilon_{\text{C}} + \epsilon_{\text{D}} \cdot \quad -\epsilon_{\text{D}})l \tag{1}$$

where $C_0^{\cdot}$ corresponds to the initial concentration of the monoreduced complex detected after the laser pulse; ϵ_C and ϵ_D are the extinction coefficients of the Ru(II) complex and the reducing agent, whereas $\epsilon_{C^{\cdot}}$ and $\epsilon_{D^{\cdot}}$ stand for the absorption coefficients of the monoreduced complex and the monooxidized reductant formed by reaction (Eq. (1)); l corresponds to the optical path length. The spectroscopic detection of the monoreduced complex may be hindered by the absorption features of the starting material and of the oxidized reducing agent in wavelength ranges where overlapping occurs with the absorption bands of the monoreduced $C^{\cdot}$ species.

The differential transient absorption spectra obtained by flash photolysis of $Ru(TAP)_3^{2+}$, $Ru(phen)_2PHEHAT^{2+}$ and $[Ru(phen)_2]_2HAT^{4+}$ in the presence of H_2Q and mononucleotides are presented in Fig. 4 [44–46,38,59]. The corresponding absorption maxima are collected in Table 3, together with the differential absorption features obtained for other complexes of the TAP and HAT series [46].

The differential spectrum recorded for the mononuclear homoleptic $Ru(TAP)_3^{2+}$ complex in the presence of H_2Q (reaction (Eq. (2))) is characterized by a long wavelength shoulder ($\lambda > 500$ nm) due to LC transitions of the monoreduced $TAP^{\cdot}$ ligand. Absorption from 500 nm down to 470 nm results from MLCT transitions of the monoreduced complex involving intact TAP ligands.

$$[Ru(TAP)_3]^{2+*} + H_2Q \xrightarrow{k_q} [Ru(TAP)_3]^{+} + HQ^{\cdot} + H^{+} \quad (2)$$

The semiquinone $HQ^{\cdot}$ produced during the reductive quenching process (Eq. (2)), formed upon loss of one electron and one proton from H_2Q, contributes significantly to the transient absorption recorded after the laser pulse in the 370–450 nm region, in agreement with the previously reported absorption maxima of semiquinone ($\lambda_{max} = 410$ and 430 nm for the acid and basic forms of $HQ^{\cdot}$, respectively [47]).

For the dinuclear complex $[Ru(phen)_2]_2HAT^{4+}$ the characteristic features of the reduced $HAT^{\cdot 3+}$ bridging ligand are observed in the 400–500 nm region of the spectrum produced from flash photolysis with H_2Q. When $Ru(phen)_2(PHEHAT)^{2+}$ is photoreduced by H_2Q, a transient absorption appears around 550 nm. This band would originate from the addition of an electron on the HAT fragment of the PHEHAT ligand as suggested by the reduction potentials (Table 1). If this attribution is correct, the flash photolysis results would confirm the existence of an absorption band in the 550–650 nm range for the monoreduced $HAT^{\cdot 3+}$ ligand, already mentioned above (see Fig. 3). Note that this band is not observed in the case of the $[Ru(phen)_2]_2HAT^{4+}$–H_2Q system, probably as a consequence of the bleaching of the starting material around 600 nm. For the PHEHAT and dinuclear compounds, overlapping occurs in the 400–450 nm region between the HAT^{+} and $SQ^{\cdot}$ bands.

In the presence of GMP (reaction (Eq. (2′))), or even AMP for $Ru(TAP)_3^{2+}$, similar features are observed. The differential absorption obtained for $Ru(TAP)_3^{2+}$ in the presence of mononucleotides is again characterized by a long wavelength shoulder attributed to the monoreduced $TAP^{\cdot +}$ ligand and by intense bands around 470–500 nm due to MLCT transitions involving the unchanged ligands. The fact

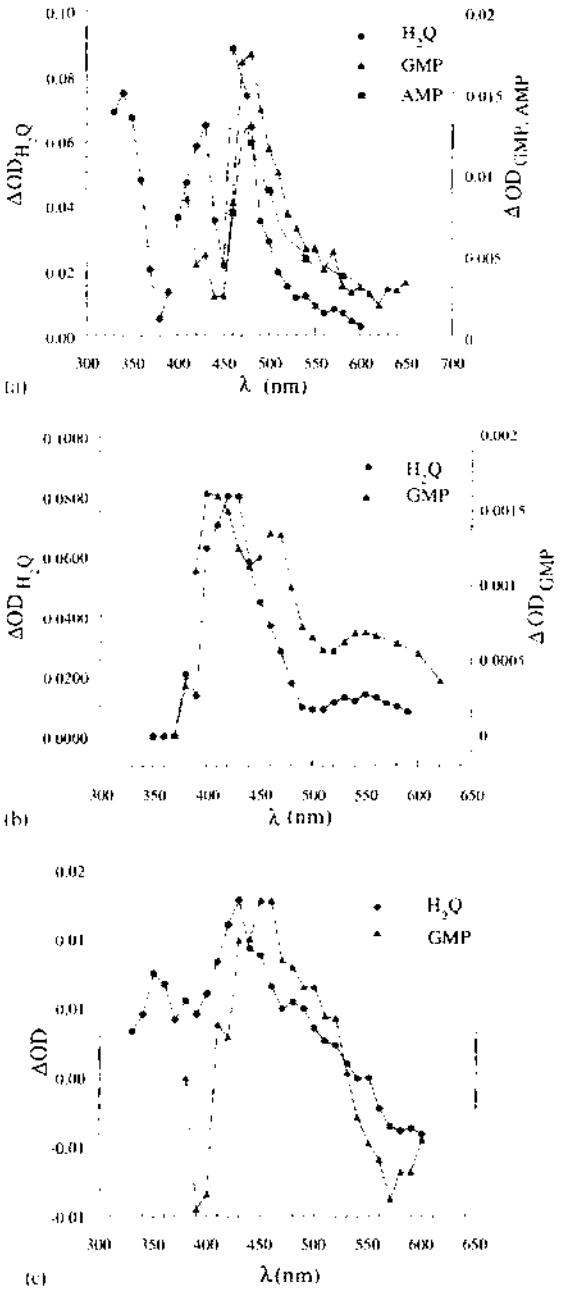

Fig. 4. Differential transient absorption spectra recorded by laser flash photolysis of various Ru(II) complexes in the presence of hydroquinone and mononucleotides. (a) Laser flash photolysis of $Ru(TAP)_3^{2+}$ in the presence of H_2Q, GMP and AMP (spectrum recorded 1 μs after the laser pulse) [adapted from Ref. [45]]. (b) Laser flash photolysis of $Ru(phen)_2PHEHAT^{2+}$ in the presence of H_2Q and GMP (spectra recorded 4 and 5 μs after the laser pulse) [adapted from Ref. [38]]. (c) Laser flash photolysis of $[Ru(phen)_2I_2HAT]^{+}$ in the presence of H_2Q and GMP (spectrum recorded 2 μs after the laser pulse) [adapted from Ref. [59]].

Table 3
Maxima for the transient absorption spectra obtained from flash photolysis in the presence of GMP, AMP and H_2Q

Complex	GMP		AMP		H_2Q	
	λ_{max} (nm)	Ref.	λ_{max} (nm)	Ref.	λ_{max} (nm)	Ref.
$Ru(HAT)_3^{2+}$	470[a]	[46]	480[a]	[46]		
$Ru(HAT)_2(TAP)^{2+}$	480[a]	[46]	470[a]	[46]		
$Ru(TAP)_2(HAT)^{2+}$	480[a]	[46]	470[a]	[46]		
$Ru(TAP)_3^{2+}$	475[a]	[45,46]	480[a]	[45,46]	425[e]	[44]
$Ru(TAP)_2(DPPZ)^{2+}$	490[b]	[126]				
$Ru(HAT)_2(bpy)^{2+}$	520[a]	[46]				
$Ru(bpy)(TAP)(HAT)^{2+}$	510[b]	[46]				
$Ru(TAP)_2(bpy)^{2+}$	505[b]	[46]				
$Ru(TAP)_2(phen)^{2+}$	500[b]	[46]				
$Ru(phen)_2(PHEHAT)^{2+}$	470, 540[c]	[38]			550[e]	[38]
$Ru(bpy)_2(TAP)^{2+}$					530[e]	[44]
$[Ru(phen)_2]_2HAT^{4+}$	460[c]	[59,130]			425[e]	[44]

[a] Data recorded under argon in buffered aqueous solution (complex 10^{-4}M, GMP or AMP 0.01M, phosphate buffer 0.1M, pH 7).
[b] Data recorded under the same conditions as [a], without buffer (pH 9–10).
[c] Data recorded under the same conditions as [a], with Tris buffer 0.5M, pH 7.
[d] Data recorded in argon purged solution (complex 10^{-4}M, H_2Q 0.01M).
[e] Data recorded under the same conditions as [c], with a complex concentration of 1.2×10^{-5}M and 0.03M H_2Q.
[f] Data recorded under the same conditions as [c], with a complex concentration of 5×10^{-5}M.

that the absorbance is weaker in the 370–450 nm region with GMP than with H_2Q originates of course from the absence of the intense transient absorption of $HQ^{\cdot}$.

$$[Ru(TAP)_3]^{2+} + GMP \xrightarrow{h\nu_q} [Ru(TAP)_3]^{+} + GMP^{+\cdot} - H^{+} \quad (2')$$

Similarly, the transient spectra produced with $Ru(phen)_2(PHEHAT)^{2+}$ and $[Ru(phen)_2]_2HAT^{4+}$ in the presence of GMP show an absorption around 450 nm corresponding to the monoreduced ligand. For the PHEHAT complex again, an additional transient absorption band appears in the 500–600 nm region, also characteristic of a reduction of the HAT fragment of PHEHAT.

For all these complexes absorption in the 400–500 nm region should also be attributed to $GMP^{+\cdot}$. Indeed, if the laser photolysis experiments are performed in the presence of oxygen (see below), the monoreduced complex is reoxidized by oxygen within a few microseconds and the spectrum recorded after this time corresponds to the radical cation of guanine, which confirms the formation of $GMP^{+\cdot}$ during the reductive quenching process (Eq. (2')).

In summary, although the absorption maxima are not identical in the spectra recorded upon electrochemical reduction of the complexes and by flash photolysis in the presence of a reducing agent, owing to the fact that, after the laser pulse, the

spectrum corresponds to a differential absorption, the characteristic absorption of the monoreduced TAP$^{\cdot}$, PHEHAT$^{\cdot}$ and HAT$^{\cdot}$ ligands are detected in all cases. The comparison of the spectroelectrochemical and flash photolysis results thus allows to conclude that the monoreduced complex is indeed produced after the laser pulse, according to reactions (Eqs. (2)) and ((2′)) corresponding to the $Ru(TAP)_3^{2+}$ model compound.

2.3. Kinetic characterization

The lifetime of the monoreduced complex produced by the photoinduced electron transfer can be determined from the kinetic analysis of the reoxidation process regenerating the starting material. This reoxidation process may be studied either in solution, using the flash photolysis technique, or at a semiconducting electrode in a photoelectrochemical experiment. From both methods the lifetime of the monoreduced intermediate can be determined and constitutes a parameter which allows also the identification of the electroactive reduced species as will be shown in the PEC chapter.

The laser flash photolysis technique allows us to examine the disappearance of the monoreduced species on the basis of the transient absorption decays recorded after the laser pulse. The transient decays are usually monitored at the absorption maximum of the monoreduced complex, determined from the differential transient absorption spectrum recorded just after the pulse. The method is limited in the short timescales by the pulse width of the laser source used in the experiments. For the results reviewed in this paper, the shortest detectable lifetimes are on the order of a few ns.

The reoxidation pathway of the monoreduced complex depends on several factors which are illustrated below in the case of the $Ru(TAP)_3^{2+}$–H_2Q and $Ru(TAP)_3^{2+}$–GMP systems. The corresponding kinetic data are summarized in Table 4.

2.3.1. Bimolecular equimolecular reoxidation processes

When flash photolysis of the $Ru(TAP)_3^{2+}$–H_2Q or $Ru(TAP)_3^{2+}$–GMP systems is conducted in deoxygenated solutions, the differential absorption disappears according to a second-order process [43,45], in agreement with the bimolecular equimolecular reoxidation of the reduced complex by the semiquinone $HQ^{\cdot}$ or radical cation $GMP^{\cdot+}$ produced during the reductive quenching process

$$[Ru(TAP)_3]^{+} + HQ^{\cdot} + H^{+} \xrightarrow{k_{2ox}} [Ru(TAP)_3]^{2+} + H_2Q \quad (3)$$

$$[Ru(TAP)_3]^{+} + GMP^{\cdot+} \xrightarrow{k_{2ox}} [Ru(TAP)_3]^{2+} + GMP \quad (3')$$

If ΔA_0 and ΔA_t are respectively the initial differential absorption and the differential absorption measured at time t, a plot of $\Delta A_0/\Delta A_t$ versus time is linear and gives a slope corresponding to the product of the second-order rate constant

Table 4
Kinetic data characterizing the monoreduced $[Ru(TAP)_3]^+$ complex produced under pulsed laser illumination of the systems $Ru(TAP)_3^{2+}$ H_2Q and $Ru(TAP)_3^{2+}$ GMP, in the absence and presence of added oxidants

System	$Ru(TAP)_3^{2+}$ H_2Q	$Ru(TAP)_3^{2+}$ H_2Q BQ			Ref.
	k_{2ox} flash[a]	k_{BQ} flash[b]	τ flash[b] $(=1/(k_{BQ}[BQ]))$	τ PEC[c]	
	$(M^{-1} s^{-1})$	$(M^{-1} s^{-1})$	(μs)	(μs)	
Kinetic data	2×10^9	2.3×10^8	55	55	[43]

System	$Ru(TAP)_3^{2+}$ GMP	$Ru(TAP)_3^{2+}$ H_2Q O_2		Ref.
	k_{2ox} flash[d]	k_{O2} flash[e]	τ flash[e] $(=1/(k_{O2}[O_2]))$	
	$(M^{-1} s^{-1})$	$(M^{-1} s^{-1})$	(μs)	
Kinetic data	1.2×10^9	0.19×10^8	40	[45,46]

[a] Derived from the transient absorption decay recorded at 480 nm by flash photolysis of a 1.1×10^{-4} M $Ru(TAP)_3^{2+}$ plus 10^{-2} M H_2Q degassed solution.
[b] Measured from the transient absorption decay recorded at 480 nm by flash photolysis of a 1.2×10^{-4} M $Ru(TAP)_3^{2+}$, 10^{-2} M H_2Q and 4×10^{-5} M BQ deoxygenated solution.
[c] Obtained from the time-evolution of the laser-induced open-circuit photopotential of an SnO_2 electrode in contact with a 10^{-2} M $Ru(TAP)_3^{2+}$, 10^{-2} M H_2Q and 4×10^{-5} M BQ deoxygenated solution (5×10^{-2} M $LiNO_3$).
[d] Derived from the transient absorption decay recorded at 470 nm by flash photolysis of a 10^{-4} M $Ru(TAP)_3^{2+}$ plus 10^{-2} M GMP Ar-saturated solution (0.1 M phosphate buffer, pH 7).
[e] Measured from the transient absorption decay recorded at 470 nm by flash photolysis of a 6×10^{-5} M $Ru(TAP)_3^{2+}$, 10^{-2} M GMP and 1.25×10^{-3} M O_2 solution (0.1 M phosphate buffer, pH 7.5).

k_{2ox} with the initial concentration of the monoreduced complex, according to Eq. (II)

$$\Delta A_0/\Delta A_t = 1 + k_{2ox}[Ru(TAP)_3^+]_0 t \quad \text{(II)}$$

As the initial concentration of the monoreduced complex $[Ru(TAP)_3^+]_0$ depends on experimental parameters such as the laser pulse intensity, the decay time derived from the slope of the $\Delta A_0/\Delta A_t$ plot has no physical meaning. The second-order rate constant k_{2ox} may however be extracted from the $\Delta A_0/\Delta A_t$ plot on the basis of Eq. (III). This equation allows evaluation of the initial concentration of $Ru(TAP)_3^+$, provided that the absorption of the reducing agent and of its oxidized form may be neglected at the wavelength where the absorption decay has been recorded.

$$[Ru(TAP)_3^+]_0 = \Delta A_0/[(\epsilon_{Ru(TAP)_3^+} - \epsilon_{Ru(TAP)_3^{2+}})l] \quad \text{(III)}$$

The determination of the initial concentration of the monoreduced complex from Eq. (III) requires the knowledge of the extinction coefficient of the monoreduced

species at the analysis wavelength. The corresponding value may be obtained from pulse radiolysis experiments [45,46,54]. On the basis of the pulse radiolysis data recorded for $Ru(TAP)_3^{2+}$ ($\epsilon_{Ru(TAP)_3^{2+}} = 8.5 \times 10^3 M^{-1} cm^{-1}$), approximate values of $2 \times 10^9 M^{-1} s^{-1}$ and $1.5 \times 10^9 M^{-1} s^{-1}$ are obtained respectively for the second-order rate constant associated with the reoxidation of the monoreduced $Ru(TAP)_3^{+}$ species by $HQ^{\cdot}$ and $GMP^{\cdot}$. Knowing the ϵ values for the monoreduced $Ru(TAP)_3^{+}$ species, the quantum yield of cage escape of the reduced complex from the ion-pair formed by the electron transfer has been calculated and is equal to 0.30 with GMP [46].

In conclusion, this discussion of the laser flash photolysis data demonstrates that the extraction of kinetic data from experiments performed in deoxygenated solutions is not straightforward. One can easily imagine that this should be still more complicated in PEC experiments as will be explained later. Therefore the kinetic behavior of monoreduced complexes is also studied in other experimental conditions illustrated in the following paragraph.

2.3.2. *Pseudomonomolecular reoxidation processes*

When an oxidizing agent such as benzoquinone (BQ) is purposely added to the $Ru(TAP)_3^{2+}$ H_2Q solution in sufficiently large amounts ($[BQ] \geq 2 \times 10^{-5} M$), the transient absorption decay becomes pseudomonomolecular and the corresponding rate constant k_{ps} depends linearly on the benzoquinone concentration [43]. In these conditions, the monoreduced complex is reoxidized by the added oxidant according to reaction (Eq. (4))

$$[Ru(TAP)_3]^{+} + BQ + H^{+} \xrightarrow{k_{ps}\,s^{-1}/[BQ]} [Ru(TAP)_3]^{2+} + HQ^{\cdot} \qquad (4)$$

The lifetime of the monoreduced complex, defined as the reciprocal value of the pseudomonomolecular rate constant k_{ps} ($\tau = 1/k_{ps}$), may be varied by adjusting the concentration of the added oxidant ([BQ]). A lifetime of 55 μs is measured for the monoreduced $Ru(TAP)_3^{+}$ in the presence of $4 \times 10^{-5} M$ of BQ. For the $Ru(TAP)_3^{2+}$ GMP system, the decay of the transient reduced complex also becomes pseudomonomolecular in oxygen-saturated solutions [45].

It should be noted however that a competition occurs between reoxidation pathways (Eq. (3)) and (Eq. (4)) when low amounts of oxidant are added to the solution: in these conditions the transient absorption decay is neither of second nor of first order. The upper limit of the oxidant concentration is given by the short time scale limit of the experimental set-up and by the possible occurrence of oxidative quenching of the excited Ru(II) complex upon oxidant addition.

3. Photoelectrochemistry (PEC)

The excited state redox properties of Ru(II) polypyridine complexes have found interesting applications in various photoelectrochemical systems. In particular, the illumination of $Ru(bpy)_3^{2+}$ [10,12,16,17,60–63] and carboxylated derivatives

such as $Ru[4,4'-(COO^-)_2bpy]_3^{4-}$ [20,64–67] or cyano derivatives like $Ru[4,4'-(COO^-)_2bpy]_3(CN)_2^{4-}$ [22], which behave as powerful reducing agents in the excited state, induces a photo-oxidation current on high band gap n-type semiconductors, such as n-doped SnO_2 electrodes or highly porous TiO_2 semiconductors [15,19,23]. This sensitization process has been shown to result from the direct injection of an electron from the excited complex adsorbed on the electrode surface into the conduction band of the semiconductor. As shown in Fig. 5, the oxidation potential of excited $Ru(bpy)_3^{2+*}$ is indeed more negative than the flat band potential of SnO_2 and is therefore located above the lower level of the SnO_2 conduction band.

Energy levels considerations show that the donor level of the excited sensitizer lies actually well above the SnO_2 conduction band edge so that the electron injection is rather favourable [68]. This interfacial elementary process where the excited complex behaves as an electron donor has been examined thoroughly by different teams: various approaches have been used including the covalent linking of the Ru(II) complex to the electrode [13,14,18,22,69–72] and, more recently, the design of supramolecular devices based on cyanobridged polymetallic compounds [21, 73–75].

In contrast to $Ru(bpy)_3^{2+}$, no efficient direct photoelectron injection into the semiconductor takes place with excited complexes such as $Ru(TAP)_3^{2+}$ and other complexes of Table 1, which exhibit a poor reducing power [42,76,77]. The donor level of their ^3MLCT excited state is indeed approximately at the same level as the SnO_2 conduction band edge. A photo-oxidation current is however measured on SnO_2 under illumination of $Ru(TAP)_3^{2+}$ in the presence of a reductive quencher such as hydroquinone [42]. This photocurrent is qualified as supersensitized and the hydroquinone is referred to as the supersensitizer. The electroactivity, i.e. the origin of this photocurrent, is quite different from the direct photoelectron injection process described above for $Ru(bpy)_3^{2+}$ and its derivatives; it is attributed in this case to the

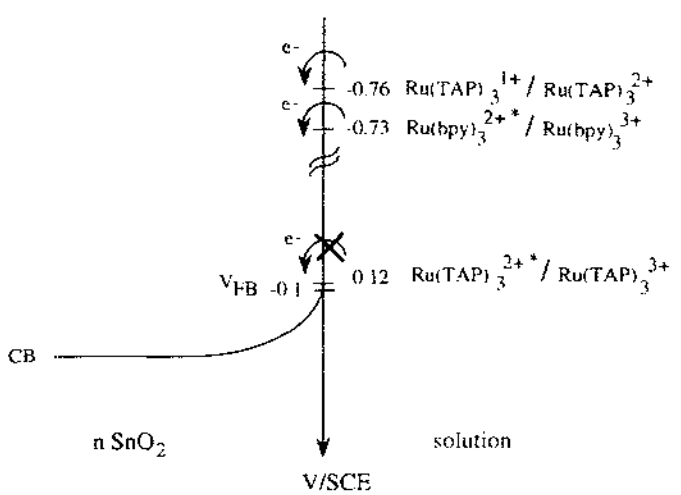

Fig. 5. Energy level diagram of the SnO_2–$Ru(TAP)_3^{2+}$ and SnO_2–$Ru(bpy)_3^{2+}$ solution interfaces.

monoreduced complex photogenerated transiently in the bulk solution by the reductive quenching process (reaction (Eq. (1))). The so-formed $Ru(TAP)_3^+$ species is indeed particularly reducing ($E_{Ru^{3+}/Ru^{2+}}$ = 0.76 V vs SCE [42]) so that, in contrast to the excited $Ru(TAP)_3^{2+*}$, it is able to inject an electron into the SnO_2 conduction band, whose band edge is located well below the donor level of $Ru(TAP)_3^+$ (Fig. 5). The electron injection (k_i) takes place after diffusion of the monoreduced complex from the bulk solution to the electrode surface, according to reaction (Eq. (5)). The lifetime of the transient electroactive $Ru(TAP)_3^+$ species diffusing to the electrode is limited by the bulk chemistry involving back electron transfer (reaction (Eq. (3))) and potential scavenging by oxidants (benzoquinone or oxygen, reaction (Eq. (4))) which would be present in solution.

$$\{Ru(TAP)_3\}^{1+} \rightsquigarrow [Ru(TAP)_3]^{+}{}_{electrode} \xrightarrow{k_i} [Ru(TAP)_3]^{2+} + 1e_{CB} \qquad (5)$$

This supersensitization process of semiconducting electrodes by oxidizing Ru(II) complexes illuminated in the presence of a reductant can actually be examined by two types of measurements: (i) stationary photocurrents recorded under continuous irradiation and (ii) time-resolved measurements of open-circuit photopotentials induced under pulsed irradiation. Both methods are briefly described below, together with the useful parameters extracted from the corresponding experimental data. A comparison is made with the results obtained from the other techniques discussed above for the study of transiently produced monoreduced species.

3.1. Steady-state PEC experiments

In this type of experiment, the Ru(II) complex reductant solution is illuminated through the transparent SnO_2 electrode of the electrochemical cell with a continuous light source: the resulting stationary photo-oxidation current, reached after a fast initial rise, is measured for various polarization potentials applied to the semiconductor. As outlined below, this method under continuous illumination allows us to confirm that the supersensitized photocurrent results indeed from the quenching process (Eq. (2)) followed by process (Eq. (5)) and does not find its origin in any other supersensitization mechanism described for xanthenic dyes such as Rhodamine B for example. In this latter case, the dye injects from its adsorbed excited state an electron into the SnO_2 conduction band [78–81]. The adsorbed oxidized dye which is formed is then "trapped" by hydroquinone, regenerating the starting adsorbed dye on the semiconductor.

With the oxidizing complexes discussed in this article, if electron injection at the SnO_2 electrode takes place from the transient reduced complex as described above, the steady-state photo-oxidation current measured at a given polarization potential increases as a function of the reductant concentration added to the bulk solution until a plateau value is reached. Indeed the amount of produced electroactive C^+ species depends on the efficiency of the reductive quenching process (reaction (Eq. (1))). The treatment of the corresponding data according to Eq. (IV) allows

determination of the photoelectrochemical Stern–Volmer constants K_{SV}^{PEC} [42,82,83]

$$\frac{I_\infty - I_0}{I - I_0} = 1 + \frac{1}{k_q^{PEC}\tau_0[Q]} = 1 + \frac{1}{K_{SV}^{PEC}[Q]} \qquad (IV)$$

where Q is the quencher or supersensitizer added to the solution (i.e. H_2Q). I_∞ is the plateau value of the steady-state photocurrent reached at high reductant concentration, I_0 is the photocurrent measured in the absence of quencher, k_q^{PEC} is the rate constant associated to the reductive quenching process occurring in the bulk solution and τ_0 is the lifetime of the excited Ru(II) complex measured in the absence of quencher. These Stern–Volmer constants are qualified as photoelectrochemical, in contrast to conventional Stern–Volmer constants measured from luminescence quenching experiments. Obviously, values obtained from both methods should be the same, if the postulated supersensitization mechanism is correct.

The Stern–Volmer constants K_{SV}^{PEC} extracted from the slope of the $(I_\infty - I_0)/(I - I_0)$ versus [Q] plots and the corresponding rate constants k_q^{PEC}, calculated using the luminescence lifetime τ_0 of the complex, are thus compared with the K_{SV}^{lum} and k_q^{lum} values obtained on the basis of conventional Stern–Volmer plots resulting from luminescence lifetimes measurements. The agreement between the kinetic quenching rate constants obtained from both techniques is illustrated in Table 5 for the $Ru(TAP)_3^{2+}$–H_2Q and $Ru(Me_2TAP)_3^{2+}$–H_2Q systems [42].

The PEC data recorded under continuous illumination confirm thus the postulated nature of the supersensitization process, discarding the occurrence of other supersensitization mechanisms previously reported for the Rhodamine B-hydroquinone system, i.e. the scavenging by hydroquinone of the oxidized dye produced after direct photoelectron injection into SnO_2, with restoration of the starting material on the electrode surface. For this "trapping" supersensitization mechanism, no agreement is found between the k_q^{PEC} and k_q^{lum} values [80].

3.2. Time-resolved PEC experiments

Although the PEC method under continuous illumination appears as a reliable technique for the kinetic study of the reductive quenching process at the origin of

Table 5
Luminescence quenching data for Ru(II) complex–H_2Q systems, derived from luminescence lifetime measurements and steady-state photoelectrochemical experiments

Complex	τ (ns)	K_{SV}^{lum} (M^{-1})	k_q^{lum} ($10^9 M^{-1} s^{-1}$)	K_{SV}^{PEC} (M^{-1}) $E = 0.1$ V	K_{SV}^{PEC} (M^{-1}) $E = 0.2$ V	k_q^{PEC} ($10^9 M^{-1} s^{-1}$) $E = 0.1$ V	k_q^{PEC} ($10^9 M^{-1} s^{-1}$) $E = 0.2$ V	Ref.
$Ru(tap)_3^{2+}$	200	990	4.9	1350	1510	6.7	7.5	[42]
$Ru(Me_2TAP)_3^{2+}$	90	470	5.2	465	521	5.1	5.7	[42]

K_{SV}^{lum} and k_q^{lum} are the Stern–Volmer constant and quenching rate constant determined from luminescence lifetime measurements, while K_{SV}^{PEC} and k_q^{PEC} are the corresponding values obtained from photoelectrochemical measurements. E is the polarization potential of the SnO_2 electrode, given in V vs SCE.

the photocurrent, it does not furnish any data on the characteristics of the electroactive species which is produced. When photoelectrochemical experiments are conducted under pulsed irradiation, information on the lifetime of the electroactive species, limited by the bulk chemistry, can be obtained. The pulsed PEC method consists of (i) irradiating with a laser pulse the Ru(II) complex–reductant solution through the transparent SnO_2 electrode of a photoelectrochemical cell and (ii) measuring the resulting open-circuit photopotential ΔV as a function of time at a 1 MΩ external resistance (oscilloscope resistance) between the small SnO_2 electrode and the large surface area Pt counter-electrode of the cell. The photopotentials may be considered as open-circuit values in the short time scales examined in these experiments, which are indeed much lower than the RC constant of the experimental system, i.e. the time needed for the electrons injected into the SnO_2 to cross the external resistance between the SnO_2 and counter-Pt electrodes.

In this type of experiment, the photopotential generated by the charging process of the semiconductor capacitance due to the electron injection has been shown to increase as a function of time until complete disappearance of the electroactive species [42,84]. If the electroactive entity corresponds to a monoreduced complex such as $Ru(TAP)_3^+$, which has a much longer lifetime than the excited complex, and which has to diffuse to the electrode surface before the electron injection occurs, the rise-time of ΔV takes place in the time scale of the lifetime of the bulk electroactive monoreduced transient.

In some particular conditions defined by the bulk chemistry, the lifetime of the electroactive monoreduced entity can be determined quantitatively from a kinetic analysis of the photopotential rise induced after the laser pulse. The lifetime determination as explained above is in particular possible in the case of a Ru(II) complex–reductant system containing a sufficiently high concentration of purposely added oxidizing agent. The bulk chemistry which limits the lifetime of the monoreduced species in this case is no longer the back electron transfer to the oxidized species formed during the reductive quenching (reaction (Eq. (3))), but corresponds to the pseudomonomolecular reoxidation process by the added oxidant (reaction (Eq. (4))). The diffusion controlled oxidation of the electroactive monoreduced complex leads, in these particular conditions, to a photopotential that increases as a function of time according to an erf function [42,43,51,84–86]

$$\Delta V(t) = (nFAC_0 \cdot C_{SC})(D/k_{ps})^{\frac{1}{2}}\mathrm{erf}(k_{ps}t)^{\frac{1}{2}} \qquad (V)$$

where n is the number of transferred electrons, F is the Faraday constant, A and C_{SC} are respectively the area and the space charge capacitance of the electrode, and D is the diffusion coefficient of the electroactive species. It should be noted that a disappearance of the monoreduced electroactive species according to a bimolecular reoxidation process in the bulk solution does not lead to an erf function for the ΔV evolution with time.

The normalization of $\Delta V(t)$ to its plateau value for a time considered as infinite gives Eq. (VI)

$$\Delta V(t)/\Delta V_\infty = \mathrm{erf}(k_{ps}t)^{\frac{1}{2}} \qquad (VI)$$

For a time t equal to the lifetime of the monoreduced complex ($\tau = 1/k_{ps}$), $\Delta V(t)/\Delta V_\infty = \mathrm{erf}(1) = 0.8427$. The time corresponding to ~84% of the ΔV plateau coincides thus with the lifetime of the electroactive species. The time domain accessible for lifetime measurements by the pulsed laser-induced PEC method is limited for the short and long times by two time constants. The short time limit [87,88] is determined by the laser pulse width and by the response time of the system, given by an RC time constant corresponding to the resistance of the cell and capacitance of the wiring system; thus, processes taking place in a time domain shorter than this rise-time cannot be examined. The limit for the long time scale is given by the RC constant controlling the discharge of the SnO_2 space charge capacitance through the external 1 MΩ resistance of the oscilloscope.

The experimental time evolution of the photopotential induced by pulsed laser irradiation at an SnO_2 electrode in contact with a $Ru(TAP)_3^{2+}$ H_2Q solution containing 4×10^{-5} M of purposely added benzoquinone is shown in Fig. 6 [43].

The time value where 84% of the ΔV plateau is reached yields a $[Ru(TAP)_3]^+$ lifetime of ~55 μs, in complete agreement with the lifetime determined from flash photolysis experiments for the same concentration of added benzoquinone (Table 4). The excellent correlation between both techniques demonstrates the utility of the laser-induced PEC method to determine lifetimes of photochemically produced transient electroactive species. The time-resolved PEC technique allows us therefore to confirm the nature of the transient electroactive species, attributed to $[Ru(TAP)_3]^+$ in the $Ru(TAP)_3^{2+}$ H_2Q system.

3.3. *Supersensitization in Nafion® films*

The supersensitization process of semiconducting SnO_2 electrodes has been investigated in particular systems where the sensitizer (i.e. the Ru(II) complex) is no longer in solution but is incorporated into a Nafion® perfluorosulphonate polymer film (Fig. 7) recast on the SnO_2 electrode, and where the supersensitizer (i.e. the reductant) diffuses freely into the polymer film from the electrolyte solution in contact with the Nafion®-coated electrode.

The loading of Ru(II) complexes in polyelectrolyte films adhering on the semicon-

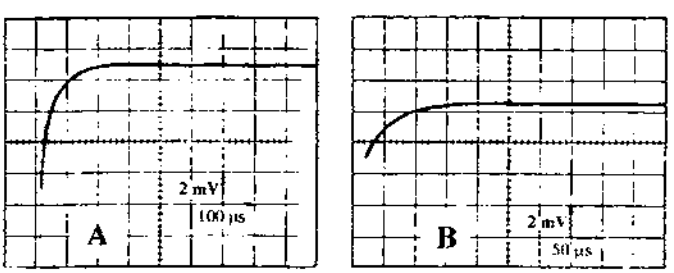

Fig. 6. Time-evolution of the laser-induced open-circuit photopotential. (A) Solution 10^{-3} M in $Ru(TAP)_3^{2+}$, 10^{-2} M in H_2Q, 2×10^{-5} M in BQ and 5×10^{-2} M in $LiNO_3$. (B) Same as (A) but with 4×10^{-5} M BQ. Dark SnO_2 potential = +0.28 V/SCE [adapted from Ref. [43]].

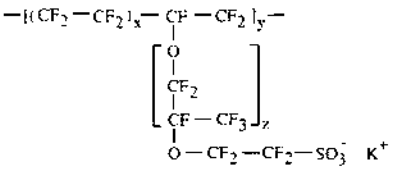

Fig. 7. Structure of the Nafion® polymer.

ductor allows to concentrate the metal compound onto the electrode surface. The concentration of the metal compound in the film can indeed reach much higher values than the concentration in the solution used to load the film. Hence, larger photocurrents may be obtained at the coated electrode than at the bare electrode under similar conditions, as previously reported for $Ru(bpy)_3^{2+}$ incorporated into a Nafion® film [89,90]. This type of system is therefore particularly attractive in the case of Ru(II) complexes such as the dinuclear compound $[Ru(phen)_2]_2HAT^{4+}$ for which much smaller amounts of material can be prepared than for simple monometallic complexes.

The $[Ru(phen)2]_2HAT^{4+}$ H_2Q system induces the same supersensitization process as that described by reactions (Eq. (2)) and (Eq. (5)) for the mononuclear $Ru(TAP)_3^{2+}$ complex. The excited dinuclear compound is indeed reductively quenched by H_2Q in solution according to the electron transfer process (Eq. (1)) [44]. Although less reducing than $Ru(TAP)_3^{+}$, the so-formed monoreduced dinuclear species ($E_{ox} = -0.49$ V vs SCE [44]) is able to inject electrons in the SnO_2 conduction band. The use of $[Ru(phen)_2]_2HAT^{4+}$ as sensitizer in solution would however require high concentrations ($> 10^{-2}$M) to observe a photocurrent or a photopotential at the SnO_2 electrode [83], which illustrates the interest of Nafion® coatings concentrating the compound on the electrode surface.

The kinetics of the reductive quenching process and the lifetime domain of the electroactive species photogenerated in the Nafion® film have been examined on the basis of steady-state and time-resolved PEC experiments. PEC methods are particularly useful for the study of this system because the flash photolysis technique is not easily adaptable for the examination of polymer films [83]. Comparison of the PEC results obtained in the polyelectrolyte film with the corresponding data obtained from the solution studies provides insights for the influence of the polymer film on the kinetics of the system, as illustrated below in the case of the $Ru(TAP)_3^{2+}$-H_2Q and $[Ru(phen)_2]_2HAT^{4+}$ H_2Q systems.

3.3.1. Diffusion of the Ru(II) complexes inside the polymer film

The steady-state PEC results obtained for the mono- and dinuclear complexes loaded in Nafion® are illustrated in Fig. 8 [83].

The stationary supersensitized photocurrents are plotted as a function of the H_2Q concentration in the electrolyte solution in contact with the Nafion®-coated electrode, for a constant polarization potential of the semiconductor. The Stern–Volmer plots derived from these data lead to straight lines (see inset of Fig. 8),

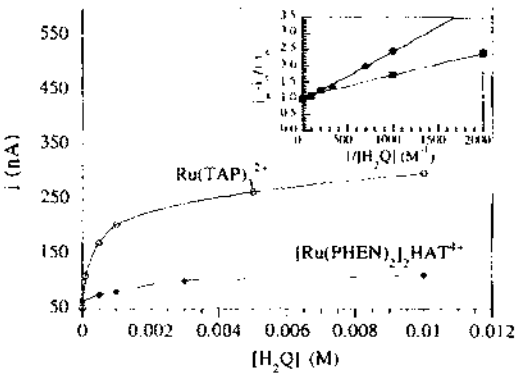

Fig. 8. Stationary photocurrents plotted versus the H_2Q concentration for $Ru(TAP)_3^{2+}$ and $[Ru(phen)_2]_2HAT^{4+}$ loaded in a Nafion® film recast on an n-doped SnO_2 electrode. The semiconductor electrode was polarized at 0.260 V versus SCE. The loading ratios (percentage of sulphonate sites of the polymer film occupied by the complex) are 33% and 24% for $Ru(TAP)_3^{2+}$ and $[Ru(phen)_2]_2HAT^{4+}$, respectively. The PEC cell is filled with a 0.1M KNO_3 supporting electrolyte solution and H_2Q. Insert: Stern–Volmer plots determined from the stationary photocurrents measured for $Ru(TAP)_3^{2+}$ (■) and $[Ru(phen)_2]_2HAT^{4+}$ (·) [adapted from Ref. [83]].

in agreement with Eq. (IV). The photoelectrochemical Stern–Volmer constants K_{SV}^{PEC} extracted from the slopes of these plots are collected in Table 6.

In order to calculate the corresponding k_q^{PEC} quenching rate constants, as explained above for the solution studies, the excited state lifetimes of $Ru(TAP)_3^{2+}$ and $[Ru(phen)_2]_2HAT^{4+}$ inside the polyelectrolyte film need to be determined. These measurements are conducted in diffuse reflectance conditions. As SnO_2 deposited on glass is not suitable for these particular measurements, the Ru(II) complex is loaded in a Nafion® film recast on a non-luminescent silica plate, and the excited

Table 6
Steady-state PEC data for the $Ru(TAP)_3^{2+}$–H_2Q and $[Ru(phen)_2]_2HAT^{4+}$–H_2Q systems in Nafion® films recast on SnO_2

Complex	$\tau_{1(Naf)}^a$ (ns)	$\tau_{2(Naf)}^a$ (ns)	$K_{SV(Naf)}^{PECb}$ (M^{-1})			$k_{q(Naf)}^{PECc}$ ($10^9 M^{-1} s^{-1}$)			Ref.
			$E=$ 0.16 V	$E=$ 0.26 V	$E=$ 0.36 V	$E=$ 0.16 V	$E=$ 0.26 V	$E=$ 0.36 V	
$Ru(TAP)_3^{2+}$	60	360	1020	820	700	2.8	2.2	1.9	[83]
$[Ru(phen)_2]_2HAT^{4+}$	40	420	–	710	920	–	1.7	2.2	[83]

[a] Luminescence lifetimes determined by diffuse reflectance measurements from Nafion® film recast on a silica plate; the solution in contact with the film is under argon. The luminescence decays are analyzed according to a biexponential law $I(t) = A_1 e^{-t/\tau_1} + A_2 e^{-t/\tau_2}$.

[b] Stern–Volmer constants obtained from the spectroelectrochemical data for different applied potentials versus SCE (E).

[c] Quenching rate constants calculated using the luminescence lifetime $\tau_{2(Naf)}$ derived from the long decay component.

state lifetime values measured in these conditions are used for the Nafion®-coated on the SnO_2 electrode. The corresponding luminescence decays obtained under pulsed irradiation are biexponential for both complexes (Table 6). This behaviour is attributed to the existence of two distinct microenvironments characterized by different local acidities in the polymer film. The fast component of the luminescence decay results from local protonation of the Ru(II) complexes which exhibit shorter luminescence lifetimes than in non-protonating solution [91–96]. These protonated excited species located in high acidity environments are quenched only for H_2Q concentrations exceeding 10^{-2}M. Therefore, to a first approximation, only the excited complexes located in the non-acidic microenvironment, associated to the long decay component, should thus be involved in the supersensitization mechanism leading to the linear Stern–Volmer plots presented in Fig. 8. The quenching rate constants k_q^{PEC} are thus derived from the Stern–Volmer constants K_{SV}^{PEC} using the long lifetime values of the luminescence decays (τ_2). The so-obtained quenching rate constants are approximately equal to 2×10^9M^{-1}s^{-1} for both complexes in the recast Nafion® film. Comparison of these values with the quenching rate constants obtained from luminescence lifetime measurements in water indicates that the quenching rate constant has decreased by a factor of 2–3 in the polyelectrolyte film for the monometallic compound, but has remained almost unchanged for the dinuclear complex. These data provide insights into the mobility of the excited compounds throughout the polymer film as developed below.

The diffusion rate constant calculated for the $Ru(TAP)_3^{2+}$–H_2Q system in water ($\sim7.4\times10^9$M^{-1}s^{-1}) [83] is of the same order of magnitude as the quenching rate constant determined from (i) luminescence lifetime measurements and from (ii) photoelectrochemical experiments in solution ($k_q^{lum\ PEC}\sim5.7\times10^9$M^{-1}s^{-1} (Table 5)). It is thus clear that the photoelectron transfer process is diffusion controlled for the monometallic system in solution. The quenching rate constant associated to the photoinduced electron transfer process decreases in Nafion®. This drop from the solution to the Nafion® film indicates that the diffusion is slowed down in the polyelectrolyte environment.

In the case of the $[Ru(phen)_2]_2HAT^{4+}$–H_2Q system, the quenching rate constant measured in water ($k_q=2\times10^9$M^{-1}s^{-1}), which is smaller than for the monometallic complex, suggests that the photoreduction process of the dinuclear compound is probably no longer diffusion controlled in solution. This conclusion is confirmed by the absence of k_q drop from the solution to the Nafion® film where the diffusion should be slightly slowed down, as concluded from the data characterizing the monometallic compound. On the other hand, if in solution the limiting step is the rate of the electron transfer itself, in Nafion®, the slower step could still be the diffusion. In other words, the electron transfer process could become diffusion controlled in Nafion®. This is in accord with the fact that a similar quenching rate constant, corresponding to the diffusion rate constant in Nafion®, is obtained in the polymer film for the monometallic and dinuclear complexes.

As the diffusion rate constant in the polymer film is only a factor 2–3 lower than the diffusion controlled quenching rate constants in solution, it may be concluded that the mobility of the metallic complexes, even the dinuclear species, is rather high

in the polyelectrolyte environment. These results suggest that the reductive quenching process occurs in a non-constraining microenvironment of the recast Nafion® film and are in agreement with the currently accepted model for Nafion®. Ion-containing polymers such as Nafion® are known to separate, on a microscopic level, into two domains or phases, corresponding to a hydrophobic bulk polymer phase (mainly fluorocarbon) and a hydrophilic ionic cluster phase [97–99]. The latter phase is randomly distributed throughout the bulk polymer and interconnects through a system of narrow channels. Since Ru(II) complexes are partly distributed in the low density cluster phase [99] and since ion-pair formation is usually not significant in this type of polymer [100], actual diffusion of the metal compounds is expected to occur in the Nafion® film. The occurrence of mass transfer processes in Nafion® films has been previously discussed in the case of $Ru(bpy)_3^{2+}$ [89].

3.3.2. Nature of the electroactive species

The supersensitization process of the electrode by the loaded Nafion® can be further investigated by the PEC method under pulsed illumination in order to evaluate the lifetime of the electroactive species responsible for the electron injection in the semiconductor. In Table 7 are indicated the approximate rise-time values of the open-circuit photopotentials recorded after the laser pulse for the $Ru(TAP)_3^{2+}$–H_2Q and $[Ru(phen)_2]_2HAT^{4+}$–H_2Q systems in solution and in Nafion® films [83].

As explained above, these ΔV rise-times correspond to the lifetime domain of the electroactive species generated from the reductive quenching process (Eq. (2)). This lifetime is limited in this case by the bimolecular reoxidation of the monoreduced complex by the semiquinone HQ· produced during the photoelectron transfer process.

For the $Ru(TAP)_3^{2+}$–H_2Q system, the ΔV rise-time increases tremendously upon incorporation of the Ru(II) complex into the Nafion® film. This indicates that the monoreduced $Ru(TAP)_3^{+}$ species has a much longer lifetime in the polymer (~15–20 ms) than in solution (~100 μs). In other words, the back electron transfer

Table 7
Time-resolved PEC data for the $Ru(TAP)_3^{2+}$–H_2Q and $[Ru(phen)_2]_2HAT^{4+}$–H_2Q systems in Nafion® films recast on SnO_2

Complex	τ_1 water[a,b]	Ref.	τ_1 Nafion®[a,b]	Ref.
$Ru(TAP)_3^{2+}$	~100 μs	[43]	~15–20 ms	[83]
$[Ru(phen)_2]_2HAT^{4+}$	~20 ms	[83]	~15–20 ms	[83]

[a] Rise times determined from pulsed laser-induced photopotentials measured as a function of time for $Ru(TAP)_3^{2+}$ and $[Ru(phen)_2]_2HAT^{4+}$ in aqueous solution and in Nafion® films recast on SnO_2, under argon. Measurements were performed in the presence of 10^{-2} M H_2Q and 0.2 M KNO_3 as supporting electrolyte.

[b] As the degassing process of a PEC cell with Nafion® swollen with water is not totally efficient and as the measurements in the presence of BQ are not reliable for non-degassed solutions, only approximate rise times were obtained from the photopotentials recorded in the absence of BQ.

from the reduced complex to $HQ^{\cdot}$ is considerably slowed down in the Nafion® film; this result may be attributed to some microenvironment effects on the semiquinone or on the reduced complex, which do not exist for the starting $Ru(TAP)_3^{2+}$ and H_2Q species as they can diffuse freely in the Nafion®.

The results obtained for the $[Ru(phen)_2]_2HAT^{4+}$–H_2Q system indicate that slow ΔV rise-times in the millisecond timescale (15–20 ms) are not only observed in Nafion®, but also in solution. This particular behaviour, which contrasts with the data obtained for the $Ru(TAP)_3^{2+}$ H_2Q system, could be attributed to the existence of a long-lived electroactive transient, which would be different from the monoreduced complex. This transient, also detected by laser flash photolysis experiments in solution [44], is proposed to be the bireduced biprotonated dinuclear complex $[Ru(phen)_2]_2HATH_2^{4+}$ which would be formed by dismutation of the protonated monoreduced complex. This last result illustrates the ability of the pulsed PEC method to obtain information on the nature of the electroactive entity on the basis of lifetime values determined from photopotential rise-times, in particular when the electroactive species does not correspond to the monoreduced complex.

4. Photophysical and photochemical behaviour in the presence of nucleic acids

The knowledge of the different properties and behaviour of the photo-oxidizing complexes listed in Table 1, discussed in the previous chapters on the basis of flash photolysis, spectroelectrochemistry and steady-state or time-resolved photoelectrochemistry experiments, leads to particularly interesting applications related to the study of biological molecules such as nucleic acids. In this final chapter, we thus highlight this particular aspect, in connection with the systems presented in the previous sections.

Much data have been accumulated on the photoredox properties of the oxidizing complexes in the presence of different reductants. Hydroquinone was first chosen because it is a rather good reductant. However the high oxidizing power of the TAP and HAT complexes in the excited state has also permitted their use with less reducing agents, such as mononucleotides corresponding to GMP and, to a lesser extent, AMP. It was therefore expected that some of these complexes would also be able, under illumination, to abstract an electron from guanine bases of DNA. From this reasonable hypothesis, a research programme was initiated in the area of DNA studies [27–29]. On the basis of previous work on the interaction of various metal complexes with nucleic acids [101], it could indeed be foreseen that the photo-oxidizing complexes discussed in this article would interact with polynucleotides, and could therefore photoreact with DNA.

In a first step, the oxidizing complexes which were involved in a photoelectron transfer with GMP were tested in the presence of DNA and polynucleotides, in order to study the existence of a photoinduced electron transfer process with DNA. It turned out from these studies that this process does indeed occur with the most oxidizing complexes. Very interestingly, it has been shown that the photoelectron transfer is correlated with two types of DNA reactions: single-strand cleavages and

photoadducts formation of the complex on DNA [102,103]. These photoprocesses were indicated by gel electrophoresis experiments, using supercoiled closed circular plasmid DNA or radioactively labelled oligonucleotides. Surprisingly, the study of those photoreactions with some complexes and ^{32}P-labelled oligonucleotides showed that the dominant photoproduct is not a cleavage product, but the formation of a covalent adduct between the oligomer and the complex. The existence of photoadduct formation has also been indicated by UV-visible absorption spectroscopy and dialysis studies with DNA and synthetic polynucleotides. The Ru(II) complexes can thus be regarded as photoreagents versus DNA [27,28].

In the first part of this chapter we show how it is possible to rationalize this photoreactivity on the basis of the experimental data. A supplementary parameter is considered in the discussion, i.e. the importance of the geometry and size of the metal compound. Steric constraints are indeed introduced when the metal compound interacts with DNA: these geometric factors appear to govern at least partially the "Ru(II) complex DNA" interaction. The second part of the chapter is thus dedicated to various strategies allowing to modulate the interaction between the metal compounds and the double helix, while keeping the photo-oxidizing ability of the complexes. The promising future of the Ru(II) complexes discussed in this paper is finally commented in relation with their potential use as molecular tools for DNA studies, medical diagnostic agents or even new anti-tumour drugs. In this last case, the Ru(II) complexes would present an interesting alternative to the well-known cis-platin compound, whose anti-cancer activity has been extensively exploited [104–108].

4.1. Behaviour of TAP and HAT complexes in the presence of polynucleotides

The interaction of a luminescent dye with polynucleotides induces in most cases an increase of the luminescence intensity and excited state lifetime of the dye. This exaltation of the luminescence properties results from the effects of the rigidity and hydrophobicity of the DNA double helix microenvironment, and thus from partial protection of the excited dye from the aqueous solution. For the Ru(II) complexes, considerable changes in the emission properties are also observed upon addition of increasing amounts of DNA. Fig. 9 illustrates these important effects for the $Ru(bpy)_n(TAP)_{3-n}^{2+}$ ($n=0$, 1, 2, 3) series [46] considered in the previous chapters.

Depending on the nature and combination of the ligands in the complex, two different behaviour are observed. If the complex contains less than two TAP or HAT π-acceptor ligands, the luminescence is enhanced upon DNA addition. In contrast, if the complex contains at least two oxidizing ligands, the luminescence is quenched in the presence of DNA.

Correlation of this behaviour with the reduction potentials of the complexes in the excited state (Table 1) shows that upon addition of DNA quenching occurs for the most oxidizing compounds. The two types of behaviour illustrated in Fig. 9 are thus explained as follows. The luminescence increase is due, as mentioned above, to effects of the DNA microenvironment (rigidity, protection from water and from oxygen quenching). These factors decrease the efficiency of the nonradiative deactiva-

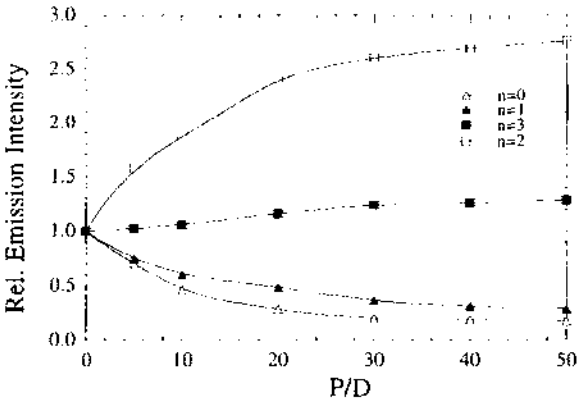

Fig. 9. Effect of increasing ratio of [DNA] (equivalent in phosphate concentration)/[complex], i.e. P/D, on the emission intensity of the complexes at constant concentration, for $Ru(bpy)_n(TAP)_{3-n}^{2+}$, $n=0$, 1, 2, 3, [adapted from Ref. [46]].

tion processes. In contrast, if the complex contains two or three oxidizing ligands, the luminescence is quenched by the nucleobases, and the correlation of this emission inhibition with the redox potentials in the excited state leads to the conclusion that the quenching would result from an electron transfer from the most reducing bases to the excited complex. To confirm this, studies have been performed with different synthetic polynucleotides (Table 8).

From examination of this table, it appears that each excited complex containing two or three oxidizing ligands is quenched in the presence of [poly(dG–dC)]$_2$. On the other hand, in the presence of [poly(dA–dT)]$_2$, the luminescence of these same compounds increases upon addition of polynucleotide, except for the most oxidizing compounds ($E^*_{red} \geq 1.4$ V vs SCE). In that particular case, the luminescence is also

Table 8
Effect of increasing concentrations of various polynucleotides on the luminescence intensity at a fixed wavelength

Complexes	CT-DNA	[poly(dG–dC)]$_2$	[poly(dA–dT)]$_2$	Reference
$Ru(bpy)_2(TAP)^{2+}$	↑		↑	[102,132]
$Ru(bpy)(TAP)_2^{2+}$	↓		↑	[102]
$Ru(TAP)_3^{2+}$	↓	↓	↑	[45,102]
$Ru(bpy)(HAT)_2^{2+}$	↓		↑	[46,133]
$Ru(HAT)_3^{2+}$	↓		↓	[46,132]
$Ru(bpy)(TAP)(HAT)^{2+}$	↓		↑	[132]
$Ru(TAP)_2(HAT)^{2+}$	↓	↓	↑	[132]
$Ru(TAP)(HAT)_2^{2+}$	↓		↓	[132]
$Ru(phen)_2(PHEHAT)^{2+}$	↑		↑	[38]
$Ru(phen)_2(DPPZ)^{2+}$	↑		↑	[38]
$Ru(TAP)_2(DPPZ)^{2+}$	↓		↑	[126]
$[Ru(phen)_2]_2HAT^{4+}$	↑		↑	[59,134]

quenched in the presence of [poly(dA–dT)]$_2$. In other words, for all the complexes for which a photoinduced electron transfer has been demonstrated with GMP, luminescence quenching is detected with DNA or [poly(dG–dC)]$_2$ and luminescence enhancement is observed in the presence of [poly(dA–dT)]$_2$. In the case of the most oxidizing complexes however, when a photoinduced electron transfer is indicated between AMP and the complex, the luminescence is also quenched in the presence of [poly(dA–dT)]$_2$. Surprisingly, although $Ru(TAP)_3^{2+*}$ and $Ru(TAP)_2(HAT)^{2+*}$ are inhibited by AMP, they exhibit luminescence enhancement in the presence of [poly(dA–dT)]$_2$. For these two complexes, it may be possible that two antagonistic effects operate. Thus the luminescence decrease due to some adenine quenching would be more than compensated by the emission increase arising from the protection effect of the double helix. It might also be possible that the geometrical constraints generate an unfavourable orientation of the donor base and the acceptor complex so that an efficient quenching is prevented, in contrast with the situation observed in the presence of AMP.

In summary, the experiments performed with synthetic polynucleotides can be correlated with emission quenching by the mononucleotides. This suggests that with DNA, the luminescence inhibition would operate by electron transfer via the guanines (also via the adenines for the most oxidizing complexes). In order to confirm these conclusions, laser flash photolysis experiments have been carried out with the complexes in the presence of DNA. As outlined above in the case of hydroquinone or GMP as reductants, the corresponding monoreduced complex is also detected in the presence of DNA. However, as compared with the results obtained in the presence of mononucleotides, the transients which are formed with DNA are rather weak. This could originate from an important and rapid back electron transfer from the monoreduced complex to the oxidized base on the polynucleotide. Indeed when the transients resulting from the electron transfer are produced on DNA, after the laser pulse, they cannot diffuse away as they do in the "Ru(II) complex–mononucleotide" systems.

Other interesting experiments have been conducted with DNA in order to observe the protection effect of the DNA microenvironment not only on the excited complex, as discussed above, but also on the transient monoreduced complex produced in situ, on the DNA. In order to show this particular aspect, the "complex–hydroquinone–benzoquinone" system, described in many details in the PEC section, has been used to probe the protection effect of the DNA double helix on the transient monoreduced complex. The complex and polynucleotide which have been chosen for this study are the $Ru(TAP)_2(HAT)^{2+}$ and [poly(dA–dT)]$_2$ where no luminescence quenching of the complex is observed. Thus when hydroquinone 50 mM and benzoquinone 1 mM are added to this complex in interaction with [poly(dA–dT)]$_2$, pulsed illumination of the solution induces a quenching of the excited complex by H_2Q, comparable to the process described in reaction (Eq. (2)). At this stage a first effect of DNA protection is observed. Indeed the k_q value for the inhibition process is lower ($1 \times 10^9 M^{-1} s^{-1}$) in the presence of [poly(dA–dT)]$_2$ than when the polynucleotide is omitted ($3.5 \times 10^9 M^{-1} s^{-1}$). On the other hand, just after the laser pulse, the pseudo first-order disappearance of the monoreduced

complex corresponding to reoxidation by benzoquinone (reaction (Eq. (4))) can be followed. At this level, a second effect of the DNA protection is observed, i.e. on the lifetime of the transient monoreduced complex. Without $[poly(dA–dT)]_2$ the decay is indeed faster than in the presence of $[poly(dA–dT)]_2$ (both in the time scale of a few μs). These experiments demonstrate thus that a transient monoreduced complex produced in situ on the DNA is also protected by the double helix.

4.2. DNA reactions or damage induced by the photoelectron transfer

Single strand cleavages of plasmid DNA upon excitation of a Ru(II) complex interacting with the plasmid have been observed for $Ru(phen)_3^{2+}$ and $Ru(bpy)_3^{2+}$ [109–111]. The quantum yields of these cleavages are however very low [112] and have been proposed to originate from oxygen singlet sensitization by the complex [113]. In contrast, higher quantum yields of cleavage are observed in the presence of oxidizing ruthenium complexes of TAP, HAT and BPZ [27]. This is clearly shown in Fig. 10 for the series of complexes $Ru(bpy)_n(TAP)_{3-n}^{2+}$ and $Ru(bpy)_n(HAT)_{3-n}^{2+}$ ($n=0$, 1, 2, 3) [102,46]. The single strand breaks in the plasmid have been demonstrated to result from the photoelectron transfer process involving the excited complex and a guanine base of DNA. This process indeed generates a guanine radical cation in the DNA, which would abstract an H-atom from a neighbouring ribose, giving rise, after several reactions, to a final strand break [114].

On the other hand, experiments with ^{32}P-labelled oligonucleotides involving the same series of complexes show the appearance of photoadducts of the complex on DNA, for illumination times where no cleavages are detected. This photoadduct formation has been demonstrated from two types of experiments. UV/visible absorption measurements allow an easy monitoring of the formation of photoproducts with DNA under visible irradiation of the complexes. The spectroscopic changes observed in those studies indicate the tris-chelated character of the new metallic product formed upon irradiation. On the other hand, dialysis experiments indicate that these photoproducts correspond to photoadducts covalently bound to the DNA, as they are retained in the dialysis bag [46,103]. Such photoadduct formation can be correlated with the oxidizing power of the complexes in the excited state, as the photoadducts are formed only with the most oxidizing compounds. Moreover, they are produced with both double-stranded and single-stranded oligonucleotides [103]. It is proposed that the adduct results from the reaction of the monoreduced complex with the guanine radical [45], as shown in the following equations for $Ru(TAP)_3^{2+}$

$$Ru(TAP)_3^{2+} + G + h\nu \rightarrow Ru(TAP)_2(TAP^{\cdot-})^{+} + G^{\cdot+} \quad (6)$$

$$G^{\cdot+} \rightarrow G(-H)^{\cdot} + H^{+} \quad (7)$$

$$Ru(TAP)_2(TAP^{\cdot-})^{+} + H^{+} \rightarrow Ru(TAP)_2(TAPH^{\cdot})^{2+} \quad (8)$$

$$Ru(TAP)_2(TAPH^{\cdot})^{2+} + G(-H)^{\cdot} \rightarrow \text{photoadduct} \quad (9)$$

As the photoadduct formed with DNA exhibits a similar absorption spectrum as

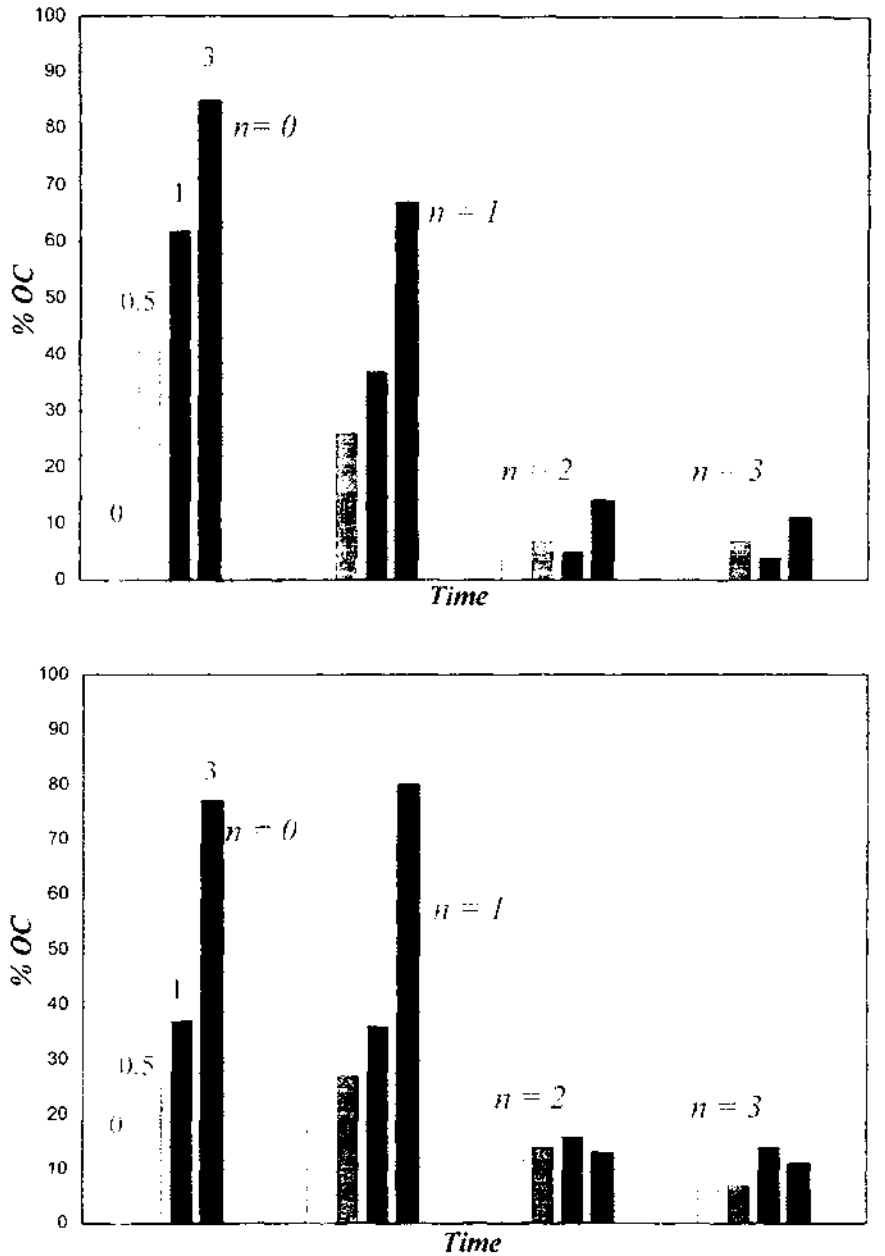

Fig. 10. Percentage of OC form on visible irradiation of the plasmid pBR322 in the presence of $Ru(bpy)_n(TAP)_{3-n}^{2+}$, $n=0, 1, 2, 3$, (P/D = 10 in 10 mM phosphate buffer, pH 7), with 0 min (dotted bars), 0.5 min (light hatch bars), 1 min (dark hatch bars) and 3 min (filled bars), of irradiation at 436 nm [adapted from Ref. [46]].

the one produced with GMP, the studies aiming to determine the structure of this photoproduct have been conducted first on the $Ru(TAP)_3^{2+}$ GMP system. After isolation of the photoadduct from the irradiated mixture with GMP, the ribose-phosphate group has been removed by acid treatment and the resulting compound characterized by NMR and electrospray mass spectrometry [115]. The corresponding structure, given in Fig. 11, shows that the guanine is covalently linked to the complex through the exocyclic NH_2 group of the base anchored to the α position of a non-chelated nitrogen of one of the TAP ligands.

More recently, photoadducts resulting from irradiation of $Ru(bpy)(TAP)_2^{2+}$ in the presence of DNA have been isolated after enzymatic and acid hydrolytic treatments of the photosensitized DNA [116]. Two isomers are formed, both resulting from the bonding of the exocyclic amino group of the guanine to one of the TAP ligands, as shown in Fig. 12. Note that the anchoring via the NH_2 position is consistent with an interaction of the complex in the minor grooves of the helix.

4.3. Modulation of the interaction with DNA

4.3.1. Complexes displaying no interaction

As mentioned in the introduction of this chapter, changes of the ligands coordinated to the metal centre do not only modify the redox properties of the resulting complex, but also influence the interaction of the metal compound with DNA. $Ru(Me_2TAP)_3^{2+}$ (see Fig. 13) represents a typical case illustrating this point [46]. This compound behaves indeed as $Ru(TAP)_3^{2+}$ if we compare the reduction potentials of their ^{3}MLCT states (Table 1), or if we consider the quenching rate constants (Table 2) obtained for both complexes with hydroquinone or GMP as reductants (see also the PEC section). However, despite an inhibition of the excited

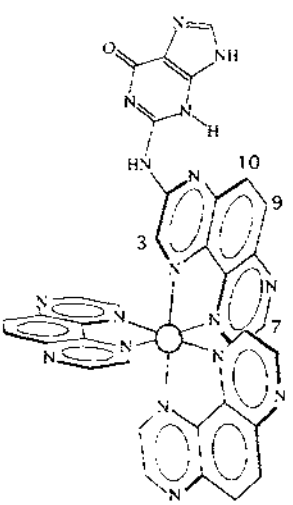

Fig. 11. Structure of the photoadduct formed under irradiation of $Ru(TAP)_3^{2+}$ and GMP, after HCl treatment to remove the ribose-phosphate.

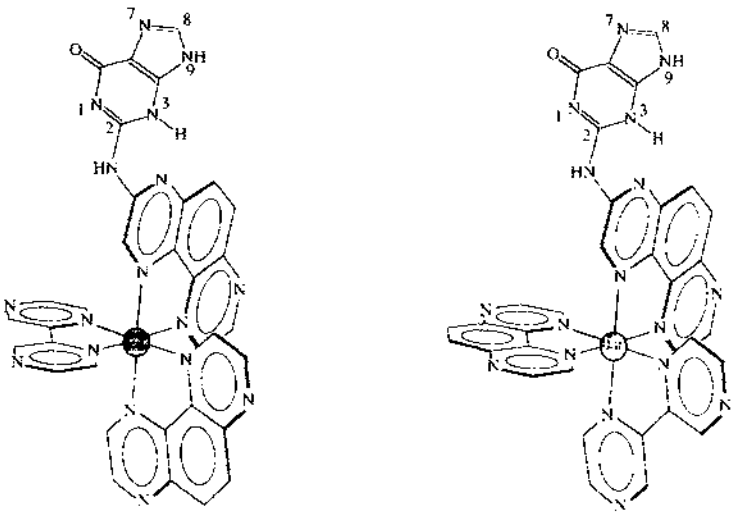

Fig. 12. Structures of the photoadducts formed under irradiation of $Ru(bpy)(TAP)_3^{2+}$ in the presence of DNA, after enzymatic and acid hydrolytic treatments of the photosensitized DNA.

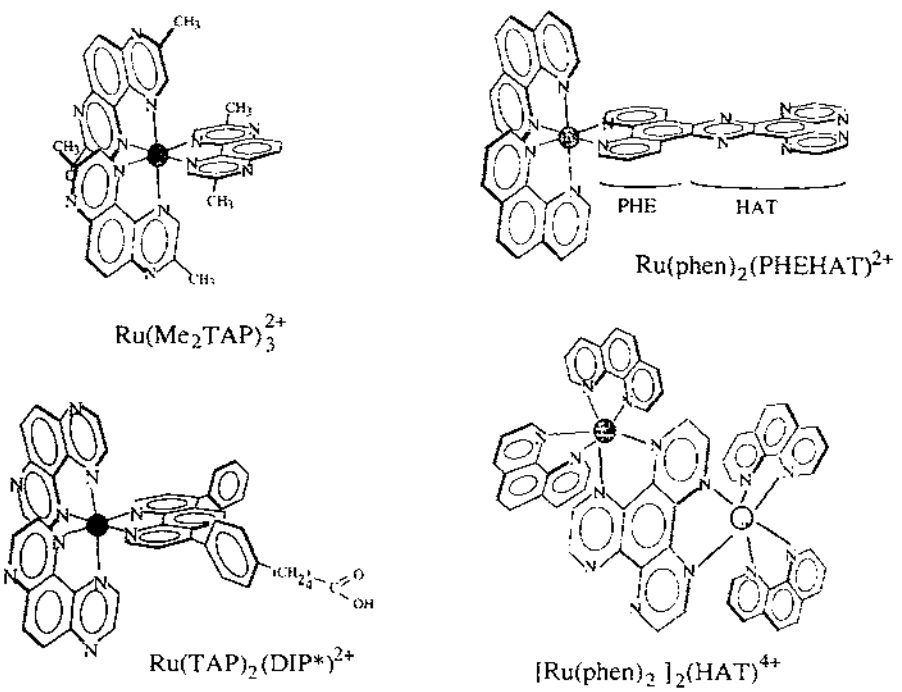

$Ru(Me_2TAP)_3^{2+}$

$Ru(phen)_2(PHEHAT)^{2+}$

$Ru(TAP)_2(DIP^*)^{2+}$

$[Ru(phen)_2]_2(HAT)^{4+}$

Fig. 13. Structure of complexes exhibiting special interactions with DNA.

$Ru(Me_2TAP)_3^{2+}$ by GMP, neither absorption nor emission changes are observed upon CT-DNA addition. This lack of luminescence quenching by DNA, not expected for such a photo-oxidizing complex, is attributed to a poor interaction with the polynucleotide, resulting from steric hindrance of the methyl groups with the double helix backbone.

4.3.2. Complexes with extended planar ligands

Although the photo-oxidizing power of the Ru(II) complexes involved in electron transfer causing DNA damages makes them attractive for different applications (see further), several problems related to these complexes remain to be solved. For example their relatively weak binding constants to DNA represent limiting factors preventing their direct application in biology. One strategy allowing us to solve this problem consists in preparing complexes which are able to intercalate one of their ligands between the base pairs of the DNA double helix. This approach led to the preparation of an extended planar ligand, the dipyrido[3,2-*a*:2′,3′-*c*]phenazine or DPPZ [41], and the corresponding $Ru(bpy/phen)_2(DPPZ)^{2+}$ complexes [117–124]. However, even if it has been demonstrated that these complexes display a high affinity for DNA, they are not photoreactive versus DNA. Indeed they are not sufficiently oxidant in their excited states to induce a photoelectron transfer in the presence of mononucleotides or polynucleotides. Therefore, in order to combine in the same complex the intercalation ability with a high photo-oxidizing power, other complexes have been synthesized, such as $Ru(BPZ/TAP)_2(DPPZ)^{2+}$ [125,126], $Ru(phen)_2(PHEHAT)^{2+}$ [38] and, very recently, $Ru(TAP)_2(PHEHAT)^{2+}$ [127] (Fig. 13).

For the $Ru(BPZ/TAP)_2(DPPZ)^{2+}$ compounds, the photoreactivity originates from the introduction of two π-acceptor TAP or BPZ ligands, while keeping a good interaction via the extended DPPZ intercalator [33,125]. For $Ru(phen)_2(PHEHAT)^{2+}$, it has been shown that the PHEHAT ligand confers to the complex a very high affinity for the DNA double helix. Moreover, flash photolysis experiments have demonstrated that this ligand makes the complex sufficiently oxidizing in the excited state to abstract an electron from GMP (Fig. 4(b)) [38]. However, the oxidation process of guanines has not been observed with DNA. This situation is thus similar to that described above for $Ru(TAP)_3^{2+}$ and $Ru(TAP)_2(HAT)^{2+}$ with AMP versus $[poly(dA\text{–}dT)]_2$ [128]. In order to make the PHEHAT complex more oxidizing in its excited state, the nature of the ancillary ligands has been changed. The resulting $Ru(TAP)_2(PHEHAT)^{2+}$ complex has proven to be a good photoreagent versus DNA as its luminescence is strongly quenched upon addition of increasing amounts of DNA [129]. Moreover this photo-oxidizing complex shows, as expected for a complex based on an extended planar ligand, a high affinity for DNA. In other words, this new complex combines the interaction efficiency with the photoreactivity versus DNA.

4.3.3. Anchoring of complexes to synthetic oligonucleotides

In order to target the interaction, and thus the formation of photoadducts, on specific DNA sequences, photoreactive complexes have been chemically anchored

to synthetic oligonucleotides. This strategy has been adopted with a TAP complex which has been derivatized (see Fig. 13) and chemically attached, through the 5-position of a thymidine base, to an oligonucleotide sequence complementary to a target sequence [33,126,130]. Very interestingly, it has been shown that the luminescence of the anchored complex is quenched when the Ru-derivatized oligonucleotide is hybridized with the complementary sequence, and this only if the target sequence contains guanines in the vicinity of the attached complex. This indicates that a photoelectron transfer takes indeed place from those guanines to the attached excited complex. Moreover, the existence of such a quenching process is correlated with an irreversible photo-crosslinking of the two strands, indicated by gel electrophoresis, and which originates from the formation of a photoadduct of the attached complex on the complementary strand.

These results open interesting perspectives for the use of this type of Ru(II) compounds as new anti-tumour or anti-viral drugs, in the context of anti-gene and anti-sense strategies aiming to inhibit the expression of specific DNA and RNA sequences.

4.3.4. Bimetallic complexes

In order to improve the selectivity in the complex–DNA interaction, other research has been focused on the design of complexes which target particular DNA topologies. In this context, the bimetallic complex based on the bridging HAT ligand [131,39], already discussed in the previous sections, appears to be a novel, attractive and interesting DNA photoreagent (see Fig. 13). Indeed, $[Ru(phen)_2]_2HAT^{4+}$ has been shown to interact exclusively with denatured DNA [59]. This DNA can be considered to be formed of 60% of normal double helix portions, and 40% of portions where the two strands are separated. Because of its size the dinuclear complex cannot penetrate inside the grooves of the normal DNA double helix but, in contrast, the denatured portions are accessible to the dinuclear compound. Moreover, its four positive charges induce a high affinity for the DNA strands. It has also been shown by laser flash photolysis that the dinuclear complex undergoes a reductive quenching process with GMP (Fig. 4(c)) and guanine-containing polynucleotides. In correlation with this electron transfer process a photoadduct has indeed been observed with GMP. However, with DNA, probably because of important steric hindrance preventing a good contact of the complex with the DNA bases, the photoelectron transfer process does not lead to the formation of a photoadduct. There is nevertheless one exception which corresponds to the illumination of the dinuclear complex with denatured DNA. In that case, as mentioned above, the complex can probably more easily approach the nucleobases at the level of the denatured portions and thus produce a photoadduct.

In conclusion it seems that these bimetallic complexes could be used for the detection of single stranded DNA portions in irregular DNA structures. This illustrates another application of the complexes for DNA studies, i.e. as molecular tools in order to probe the DNA structures or topologies.

5. Conclusion

In this review article, we have shown, for a series of photo-oxidizing Ru(II) complexes (Table 1), based mainly on the TAP and HAT ligands, that the knowledge of their behaviour with different reductants, investigated with quite different methods and techniques in spectroelectrochemistry, photoelectrochemistry and flash photolysis, leads to interesting developments of these compounds for the study of DNA, as emphasized in the final DNA chapter. Thus as illustrated above, one can easily imagine the important role which could be played by these complexes in the future, for example as molecular tools for the study of DNA. Some of these tools could also be applied in medical diagnostics, to detect special DNA topologies generated by some mutations. Moreover, preliminary experiments have shown that some TAP complexes are able to inhibit the transcription of DNA into RNA, in artificial biological systems. These observations may thus leave hope for the use of such compounds as anti-cancer drugs activated under visible illumination.

Acknowledgements

A.K.D. and C.M. are grateful to the SSTC ("Pôles d'attraction interuniversitaires", PAI-IUAP, 4/11) for financial support. The COST D1 programme is also gratefully acknowledged.

References

[1] G.M. Brown, S.-F. Chan, C. Creutz, H.A. Schwarz, N. Sutin, J. Am. Chem. Soc. 101 (1979) 7638.
[2] M. Kirch, J.-M. Lehn, J.-P. Sauvage, Helv. Chim. Acta 62 (1979) 1345.
[3] R.J. Crutchley, A.B.P. Lever, J. Am. Chem. Soc. 102 (1980) 7128.
[4] M. Neumann-Spallart, K. Kalyanasundaram, M. Grätzel, C. Grätzel, Helv. Chim. Acta 63 (1980) 1111.
[5] S.-F. Chan, M. Chou, C. Creutz, T. Matsubara, N. Sutin, J. Am. Chem. Soc. 103 (1981) 369.
[6] R.J. Crutchley, A.B.P. Lever, Inorg. Chem. 21 (1982) 2276.
[7] H. Cano-Yelo, A. Deronzier, J. Chem. Soc. Faraday Trans. I 80 (1984) 3011.
[8] S. Cosnier, A. Deronzier, N. Vlachopoulos, J. Chem. Soc. Chem. Commun. (1989) 1259.
[9] T.J. Meyer, Acc. Chem. Res. 22 (1989) 163.
[10] M. Gleria, R. Memming, Z. Phys. Chem. Neue Folge 98 (1975) 303.
[11] W.D.K. Clark, N. Sutin, J. Am. Chem. Soc. 99 (1977) 4676.
[12] T. Matsumura-Inoue, H. Tomono, M. Kasai, T. Tominaga-Morito, J. Electroanal. Chem. 95 (1979) 109.
[13] P.K. Ghosh, T.G. Spiro, J. Am. Chem. Soc. 102 (1980) 5543.
[14] J.B. Goodenough, A. Hamnett, M.P. Dave-Edwards, G. Campet, R.D. Wright, Surf. Sci. 101 (1980) 531.
[15] J. Kiwi, Chem. Phys. Lett. 83 (1981) 594.
[16] A. Kirsch-De Mesmaeker, J. Nasielski, Bull. Soc. Chim. Belg. 91 (1982) 731.
[17] K. Hashimoto, T. Sawai, T. Sakata, Nouv. J. Chim. 105 (1983) 5695.
[18] D.A. Gulino, H.G. Drickamer, J. Phys. Chem. 88 (1984) 1173.
[19] J. Desilvestro, M. Grätzel, L. Kavan, J. Moser, J. Augustynski, J. Am. Chem. Soc. 107 (1985) 2988.

[20] D.N. Furlong, D. Wells, W.H.F. Sasse, J. Phys. Chem. 90 (1986) 1107.
[21] R. Amadelli, R. Argazzi, C.A. Bignozzi, F. Scandola, J. Am. Chem. Soc. 112 (1990) 7099.
[22] T.A. Heimer, C.A. Bignozzi, G.J. Meyer, J. Phys. Chem. 97 (1993) 11987.
[23] A. Hagfeldt, M. Grätzel, Chem. Rev. 95 (1995) 49.
[24] F. Scandola, M.T. Indelli, C. Chiorboli, C.A. Bignozzi, Top. Curr. Chem. 158 (1990) 73.
[25] S. Campagna, G. Denti, S. Serroni, A. Juris, M. Venturi, V. Ricevuto, V. Balzani, Chem. Eur. J. 1 (1995) 211.
[26] I. Klimant, O.S. Wolfbeiss, Anal. Chem. 34 (1995) 3160.
[27] A. Kirsch-De Mesmaeker, J.-P. Lecomte, J.M. Kelly, Top. Curr. Chem. 177 (1996) 25.
[28] C. Moucheron, A. Kirsch-De Mesmaeker, J. Kelly, J. Photochem. Photobiol., B: Biol. to be published.
[29] C. Moucheron, A. Kirsch-De Mesmaeker, J.M. Kelly, in: J.P. Richmond (Ed.), Structure and Bonding, Springer Verlag, Berlin, submitted.
[30] J. Telser, K.A. Cruickshank, K.S. Schanze, T.L. Netzel, J. Am. Chem. Soc. 111 (1989) 7221.
[31] W. Bannwarth, W. Pfleiderer, F. Müller, Helv. Chim. Acta 74 (1991) 1991.
[32] Y. Jenkins, J.K. Barton, J. Am. Chem. Soc. 114 (1992) 8736.
[33] I. Ortmans, S. Content, A. Kirsch-De Mesmaeker, W. Bannwarth, J.-F. Constant, E. Defrancq, J. Lhomme, in preparation.
[34] H. Dürr, G. Dörr, K. Zengerle, E. Mayer, J.-M. Curchod, A.M. Braun, Nouv. J. Chim. 9 (1985) 717.
[35] M.-A. Haga, E.S. Dodsworth, G. Eryavec, P. Seymour, A.B.P. Lever, Inorg. Chem. 24 (1985) 1901.
[36] D.R. Prasad, D. Hessler, M.Z. Hoffman, N. Serpone, Chem. Phys. Lett. 121 (1985) 61.
[37] A. Masschelein, L. Jacquet, A. Kirsch-De Mesmaeker, J. Nasielski, Inorg. Chem. 29 (1990) 855.
[38] C. Moucheron, A. Kirsch-De Mesmaeker, S. Choua, Inorg. Chem. 36 (1997) 584.
[39] L. Jacquet, A. Kirsch-De Mesmaeker, J. Chem. Soc. Faraday Trans. 88 (1992) 2471.
[40] T.J. Rutherford, O. Van Gijte, A. Kirsch-De Mesmaeker, F.R. Keene, Inorg. Chem. to be published.
[41] J.-C. Chambron, J.-P. Sauvage, E. Amouyal, P. Koffi, New J. Chem. 9 (1985) 527.
[42] A. Kirsch-De Mesmaeker, D. Maetens, R. Nasielski-Hinkens, J. Electroanal. Chem. Interface Chem. 182 (1985) 123.
[43] A. Masschelein, A. Kirsch-De Mesmaeker, New J. Chem. 11 (1987) 329.
[44] L. Tan-Sien-Hee, A. Kirsch-De Mesmaeker, J. Chem. Soc. Dalton Trans. (1994) 3651.
[45] J.-P. Lecomte, A. Kirsch-De Mesmaeker, J.M. Kelly, A.B. Tossi, H. Görrer, Photochem. Photobiol. 55 (1992) 681.
[46] J.-P. Lecomte, A. Kirsch-De Mesmaeker, M.M. Feeney, J.M. Kelly, Inorg. Chem. 34 (1995) 6481.
[47] K.B. Patel, J. Willson, J. Chem. Soc. Faraday Trans. I 69 (1973) 816.
[48] P. Subramanian, G. Dryhurst, J. Electroanal. Chem. 224 (1987) 137.
[49] L.P. Candeias, S. Steenken, J. Am. Chem. Soc. 111 (1989) 1094.
[50] Q.G. Mulazzani, S. Emmi, P.G. Fuochi, M. Venturi, M.Z. Hoffman, M.G. Simic, J. Phys. Chem. 83 (1979) 1582.
[51] G.A. Heath, L.J. Yellowlees, P.S. Braterman, J. Chem. Soc. Chem. Commun. (1981) 287.
[52] P.S. Braterman, A. Harriman, G.A. Heath, L.J. Yellowlees, J. Chem. Soc. Dalton Trans. (1983) 1801.
[53] K.R. Barqawi, T.S. Akasheh, P.C. Beaumont, B.J. Parsons, G.O. Phillips, J. Phys. Chem. 92 (1988) 291.
[54] M. D'Angelantonio, Q.G. Mulazzani, M. Venturi, M. Ciano, M.Z. Hoffman, J. Phys. Chem. 95 (1991) 5121.
[55] W.A. Nevin, A.B.P. Lever, Anal. Chem. 60 (1988) 727.
[56] G.J. Kavarnos, N.J. Turro, Chem. Rev. 86 (1986) 401.
[57] Y.A. Ilan, D. Meisel, G. Czapski, Isr. J. Chem. 12 (1974) 891.
[58] D.-S. Shin, N. Doddapaneni, S.-M. Park, Inorg. Chem. 31 (1992) 4060.
[59] O. Van Gijte, Ph.D. thesis, Université Libre de Bruxelles, 1997.
[60] M. Gleria, R. Memming, Z. Phys. Chem. Neue Folge 101 (1976) 171.
[61] R. Memming, F. Schröppel, Chem. Phys. Lett. 62 (1979) 207.
[62] R. Memming, F. Schröppel, C. Bringmann, J. Electroanal. Chem. 100 (1979) 307.
[63] R. Memming, Surf. Sci. 101 (1980) 551.

[64] P. Liska, N. Vlachopoulos, M.K. Nazeeruddin, P. Compte, M. Grätzel, J. Am. Chem. Soc. 110 (1988) 3686.
[65] N. Vlachopoulos, P. Liska, J. Augustynski, M. Grätzel, J. Am. Chem. Soc. 110 (1988) 1216.
[66] B. O'Regan, J. Moser, M. Anderson, M. Grätzel, J. Phys. Chem. 94 (1990) 8720.
[67] M.K. Nazeeruddin, A. Kay, I. Rodicio, R. Humphry-Baker, E. Müller, P. Liska, N. Vlachopoulos, M. Grätzel, J. Am. Chem. Soc. 115 (1993) 6382.
[68] H. Gerischer, Angew. Chem. Int. Ed. Engl. 27 (1988) 63.
[69] S. Anderson, E.C. Constable, M.P. Dave-Edwards, J.B. Goodenough, A. Hamnett, K.R. Seddon, R.D. Wright, Nature 280 (1979) 571.
[70] M.P. Dave-Edwards, J.B. Goodenough, A. Hamnett, K.R. Seddon, R.D. Wright, Faraday Disc. Chem. Soc. 70 (1980) 285.
[71] H.D. Abruna, P. Denisevich, M. Umana, T.J. Meyer, R.W. Murray, J. Am. Chem. Soc. 103 (1981) 1.
[72] N. Vlachopoulos, P. Liska, A.J. McEvoy, M. Grätzel, Surf. Sci. 189/190 (1987) 823.
[73] M.K. Nazeeruddin, P. Liska, J. Moser, N. Vlachopoulos, M. Grätzel, Helv. Chim. Acta 73 (1990) 1788.
[74] M. Grätzel, Coord. Chem. Rev. 111 (1991) 167.
[75] B. O'Regan, M. Grätzel, Nature 353 (1991) 737.
[76] S. Nishida, Y. Harima, K. Yamashita, Inorg. Chem. 28 (1989) 4073.
[77] K. Karlsson, A. Kirsch-De Mesmaeker, J. Phys. Chem. 95 (1991) 10681.
[78] R. Memming, Photochem. Photobiol. 16 (1972) 325.
[79] H. Gerischer, F. Willig, Top. Curr. Chem. 61 (1975) 31.
[80] A. Kirsch-De Mesmaeker, P. Leempoel, J. Nasielski, Electrochim. Acta 23 (1978) 605.
[81] A. Frippiat, A. Kirsch-De Mesmaeker, J. Phys. Chem. 89 (1985) 1285.
[82] L. Tan-Sien-Hee, L. Jacquet, A. Kirsch-De Mesmaeker, J. Photochem. Photobiol., A: Chem. 81 (1994) 169.
[83] L. Tan-Sien-Hee, A. Kirsch-De Mesmaeker, J. Electroanal. Chem. 406 (1996) 147.
[84] A. Frippiat, A. Kirsch-De Mesmaeker, J. Nasielski, J. Electrochem. Soc. 130 (1983) 237.
[85] J.R. Darwent, K. Kalyanasundaram, J. Chem. Soc. Faraday Trans. II 77 (1981) 373.
[86] A. Frippiat, A. Kirsch-de Mesmaeker, J. Electrochem. Soc. 134 (1987) 66.
[87] F. Willig, K. Bitterling, K.P. Charlé, F. Decker, Ber. Bunsenges. Phys. Chem. 88 (1984) 374.
[88] F. Willig, Ber. Bunsenges. Phys. Chem. 92 (1988) 1312.
[89] C.R. Martin, I. Rubinstein, A.J. Bard, J. Am. Chem. Soc. 104 (1982) 4817.
[90] M. Krishnan, X. Zhang, A.J. Bard, J. Am. Chem Soc. 106 (1984) 7371.
[91] R.J. Crutchley, N. Kress, A.B.P. Lever, J. Am. Chem. Soc. 105 (1983) 1171.
[92] D.P. Rillema, G. Allen, T.J. Meyer, D. Conrad, Inorg. Chem. 22 (1983) 1617.
[93] A. Kirsch-De Mesmaeker, L. Jacquet, J. Nasielski, Inorg. Chem. 27 (1988) 4451.
[94] H.B. Ross, M. Boldaji, D.P. Rillema, R.P. White, Inorg. Chem. 28 (1989) 1013.
[95] K. Shinozaki, Y. Kaizu, H. Kobayashi, Inorg. Chem. 28 (1989) 2675.
[96] H. Sun, M.Z. Hoffman, J. Phys. Chem. 97 (1993) 5014.
[97] A. Steck, H.L. Yeager, Anal. Chem. 52 (1980) 1215.
[98] H.L. Yeager, B. Kipling, R.L. Dotson, J. Electrochem. Soc. 127 (1980) 303.
[99] D.A. Buttry, F.C. Anson, J. Am. Chem. Soc. 105 (1983) 685.
[100] S.R. Lowry, K.A. Mauritz, J. Am. Chem. Soc. 102 (1980) 4665.
[101] J.K. Barton, Science 233 (1986) 727.
[102] J.M. Kelly, M.M. Feeney, A.B. Tossi, J.-P. Lecomte, A. Kirsch-De Mesmaeker, Anti-Cancer Drug Design 5 (1990) 69.
[103] M.M. Feeney, J.M. Kelly, A.B. Tossi, A. Kirsch-De Mesmaeker, J.-P. Lecomte, J. Photochem. Photobiol., B: Biol. 23 (1994) 69.
[104] S. Bruhn, J. Toney, S.J. Lippard, Prog. Inorg. Chem., Bioinorg. Chem. 38 (1990) 477.
[105] W.I. Sundquist, S.J. Lippard, Coord. Chem. Rev. 100 (1990) 293.
[106] M. Sip, M. Leng, in: D.M.J. Lilley (Ed.), Nucleic Acids and Molecular Biology, vol. 7, Springer Verlag, Berlin, 1993, p. 1.
[107] M. Boudvillain, R. Dalbiès, M. Leng, in: A. Sigel, H. Sigel (Eds.), Metal Ions in Biological Systems, vol. 33, Marcel Dekker, New York, 1996, p. 87

[108] B. Lippert, in: A. Sigel, H., Sigel (Eds.), Metal Ions in Biological Systems, vol. 33, Marcel Dekker, New York, 1996, p. 105.
[109] J.M. Kelly, A.B. Tossi, D.J. McConnell, C. OhUigin, Nucleic Acids Res. 13 (1985) 6017.
[110] M.B. Fleisher, K.C. Waterman, N.J. Turro, J.K. Barton, Inorg. Chem. 25 (1986) 3549.
[111] J.M. Kelly, A.B. Tossi, D. McConnell, C. OhUigin, C. Hélène, T. LeDoan, in: P.C. Beaumont, D.J. Deeble, B.J. Parsons, C. Rice-Evans (Eds.), Free Radicals, Metal Ions and Biopolymers, Richelieu Press, London, 1989, p. 143.
[112] A.B. Tossi, J.M. Kelly, Photochem. Photobiol. 49 (1989) 545.
[113] J. Piette, J. Photochem. Photobiol., B: Biol. 11 (1991) 241.
[114] J. Cadet, in: H. Morrison (Ed.), The Photochemistry of Nucleic Acids, vol. 1, John Wiley, New York, 1990, p. 3.
[115] L. Jacquet, J.M. Kelly, A. Kirsch-De Mesmaeker, J. Chem. Soc. Chem. Commun. 9 (1995) 913.
[116] L. Jacquet, R.J.H. Davies, A. Kirsch-De Mesmaeker, J. Am. Chem. Soc. submitted.
[117] A.E. Friedman, J.-C. Chambron, J.-P. Sauvage, N.J. Turro, J.K. Barton, J. Am. Chem. Soc. 112 (1990) 4960.
[118] A.E. Friedman, C.V. Kumar, N.J. Turro, J.K. Barton, Nucleic Acids Res. 19 (1991) 2595.
[119] R.M. Hartshorn, J.K. Barton, J. Am. Chem. Soc. 114 (1992) 5919.
[120] C. Hiort, P. Lincoln, B. Nordén, J. Am. Chem. Soc. 115 (1993) 3448.
[121] C.M. Dupureur, J.K. Barton, J. Am. Chem. Soc. 116 (1994) 10286.
[122] I. Haq, P. Lincoln, D. Suh, B. Nordén, B.Z. Chowdhry, J.B. Chaires, J. Am. Chem. Soc. 117 (1995) 4788.
[123] P. Lincoln, A. Broo, B. Nordén, J. Am. Chem. Soc. 118 (1996) 2644.
[124] C.M. Dupureur, J.K. Barton, Inorg. Chem. 36 (1997) 33.
[125] C. Sentagne, J.-C. Chambron, J.-P. Sauvage, N. Paillous, J. Photochem. Photobiol., B: Biol. 26 (1994) 165.
[126] I. Ortmans, Ph.D. thesis, Université Libre de Bruxelles, 1996.
[127] C. Moucheron, A. Kirsch-De Mesmaeker, J. Phys. Org. Chem. submitted.
[128] J.P. Lecomte, A. Kirsch-De Mesmaeker, J.M. Kelly, Bull. Soc. Chim. Belg. 103 (1994) 193.
[129] C. Vandervelden, Masters thesis, Université Libre de Bruxelles, 1997.
[130] A. Kirsch-De Mesmaeker, I. Ortmans, O. Van Gijte, W. Bannwarth, Photoreactions of polyazaaromatic mono- and bimetallic Ru(II) complexes on targeted DNA sites, 30th International Conference on Coordination Chemistry, Kyoto, 1994, p. 68.
[131] A. Kirsch-De Mesmaeker, L. Jacquet, A. Masschelein, F. Vanhecke, K. Heremans, Inorg. Chem. 28 (1989) 2465.
[132] A. Kirsch-De Mesmaeker, G. Orellana, J.K. Barton, N.J. Turro, Photochem. Photobiol. 52 (1990) 461.
[133] F. de Buyl, A. Kirsch-De Mesmaeker, A. Tossi, J.M. Kelly, J. Photochem. Photobiol., A: Chem. 60 (1991) 27.
[134] O. Van Gijte, A. Kirsch-De Mesmaeker, in preparation.